Groundwater recharge areas of a volcanic aquifer system inferred from hydraulic, hydrogeochemical and stable isotope data: Mount Vulture, southern Italy

Serena Parisi · Michele Paternoster · Claus Kohfahl · Asaf Pekdeger · Hanno Meyer · Hans Wolfgang Hubberten · Giuseppe Spilotro · Giovanni Mongelli

Abstract Environmental isotope techniques, hydrogeochemical analysis and hydraulic data are employed to identify the main recharge areas of the Mt. Vulture hydrogeological basin, one of the most important aquifers of southern Italy. The groundwaters are derived from seepage of rainwater, flowing from the highest to the lowest elevations through the shallow volcanic weathered host-rock fracture zones. Samples of shallow and deep groundwater were collected at 48 locations with elevations ranging from 352 to 1,100m above sea level (a.s.l.), for stable isotope ($\delta^{18}O$, δD) and major ion analyses. A complete dataset of available hydraulic information has been integrated with measurements carried out in the present study. Inferred recharge elevations, estimated on the basis of the local vertical isotopic gradient of $\delta^{18}O$, range between 550 and 1,200m a.s.l. The isotope pattern of the Quaternary aquifer reflects the spatial separation of different recharge sources. Knowledge of the local hydrogeological setting was the starting point for a detailed hydrogeochemical and isotopic study to define the recharge and discharge patterns identifying the groundwater flow pathways of the Mt. Vulture basin. The integration of all the data allowed for the tracing of the groundwater flows of the Mt. Vulture basin.

Keywords Volcanic aquifer · Groundwater recharge/water budget · Recharge elevation · Stable isotopes · Italy

Received: 2 July 2009 / Accepted: 24 May 2010
Published online: 18 June 2010

S. Parisi (✉)
Department of Geological Sciences,
University of Basilicata,
Campus Macchia Romana, 85100, Potenza, Italy
e-mail: serena.parisi@unibas.it

M. Paternoster · G. Mongelli
Department of Chemistry,
University of Basilicata,
Campus Macchia Romana, 85100, Potenza, Italy

C. Kohfahl
Instituto Geológico y Minero de España,
Subdelegación del Gobierno, Plaza de España/Torre Norte, 41013,
Sevilla, Spain

A. Pekdeger
Institute of Geological Sciences,
Freie Universität Berlin,
Malteserstr. 74–100, Building B, 12249, Berlin, Germany

H. Meyer · H. W. Hubberten
Isotope Laboratory of the Alfred Wegener Institute for Polar
and Marine Research Unit Potsdam,
Telegrafenberg, 14473, Potsdam, Germany

G. Spilotro
Department of Structural Engineering, Geotechnical Engineering,
Engineering Geology,
University of Basilicata,
Campus Macchia Romana, 85100, Potenza, Italy

Introduction

The application of isotope-based methods has become well established for water-resource assessment, development and management in the hydrological sciences, and is now an integral part of many water quality and environmental studies (Clark and Fritz 1997; Cook and Herczeg 2000). To meet the drinking-water needs for future generations, sustainable watershed management and more detailed knowledge about recharge processes are essential. Environmental isotopes and chemical tracers are valuable tools for investigating recharge processes and groundwater-flow pathways in hydrogeological systems. Comparison of the stable isotopic compositions of precipitation and groundwater provides an excellent tool for evaluating recharge mechanisms (Clark and Fritz 1997; Jones and Banner 2003). Numerous studies using hydrochemistry and stable isotopes of water have been used to characterize recharge processes in different hydrogeological environments. For example, Barbieri et al. (2005) characterized groundwater flow

 DOI 10.1007/s10040-010-0619-8

paths and recharge elevations in a karst aquifer of central Italy by a combined study of hydrochemistry and stable isotopes (^{2}H, ^{18}O and $^{87}Sr/^{86}Sr$). Marfia et al. (2003) combined the analysis of major and minor ions, $\delta^{13}C$ and stable isotopes to investigate the origin and the hydrogeochemical evolution of surface and groundwater in a karst-dominated geologic setting in Central America.

Several investigations on the isotopic composition of rain have been carried out in volcanic areas such as East Maui, Hawaii, Cheju Island, Korea, Tahiti-Nui, French Polynesia, Mount Etna, Italy (Lee et al. 1999; Scholl et al. 2002; D'Alessandro et al. 2004) and Stromboli, Italy (Liotta et al. 2006).

The data collected previously by Paternoster et al. (2008), identify, in general terms, the groundwater isotopic characteristics within the Vulture basin (Fig. 1) in Italy, and were used in the present study. From that work, the local meteoric water line (LMWL; $\delta D‰ = 6.56\ \delta^{18}O + 4.12$) was obtained, along with the weighted local meteoric water line (WLMWL; $\delta D‰ = 4.92\ \delta^{18}O - 9.70$), computed using the mean values weighted by the rainfall amount, identifying the monthly isotopic composition of precipitation over a two-year period at rain gauge stations.

The objective of this study is to demonstrate how natural tracers, combined with hydrogeological and hydrochemical data, can be used to get a refined understanding of recharge mechanisms and recharge elevations of basin aquifers and to better understand the hydrogeochemical evolution of groundwater. The present methodology, as demonstrated by the example of the Mt. Vulture basin, constitutes a powerful tool to better define a conceptual hydrogeological model for complex hydrogeological systems. The improved understanding of groundwater flow patterns, especially within such complex volcanic and/or sedimentary environments, is fundamental for the preservation and sustainable management of water resources.

Study area

Geology

Mt. Vulture is an isolated cone (1,320 m above sea level (a.s.l.), stratovolcano-shaped, of Quaternary age, situated along the external edge of the Apennine Chain, close to the western portion of the *Bradanic foredeep* on the northeastern sector of the Basilicata region (Italy) (Fig. 1). Volcanic activity took place from the middle Pleistocene to upper Pleistocene, starting about 0.73 million years (Ma) ago and ending about 0.13 Ma ago (Brocchini et al. 1994; Buettner et al. 2006). The volcanic products consist of 700-m thickness of dominantly undersaturated silica pyroclastic deposits and subordinate lava flows arranged in radial banks with respect to the summit of Mt. Vulture (Brocchini et al. 1994; Serri et al. 2001; Giannandrea et al. 2004). The peripheral sectors of the volcanic structure are characterized by the presence of the fluvio-lacustrine deposits from Pliocene to lower Pleistocene age, with intercalations of pyroclastic layers (Fiumara di Atella Super-synthems, Giannandrea et al. 2006; Fig. 1). The

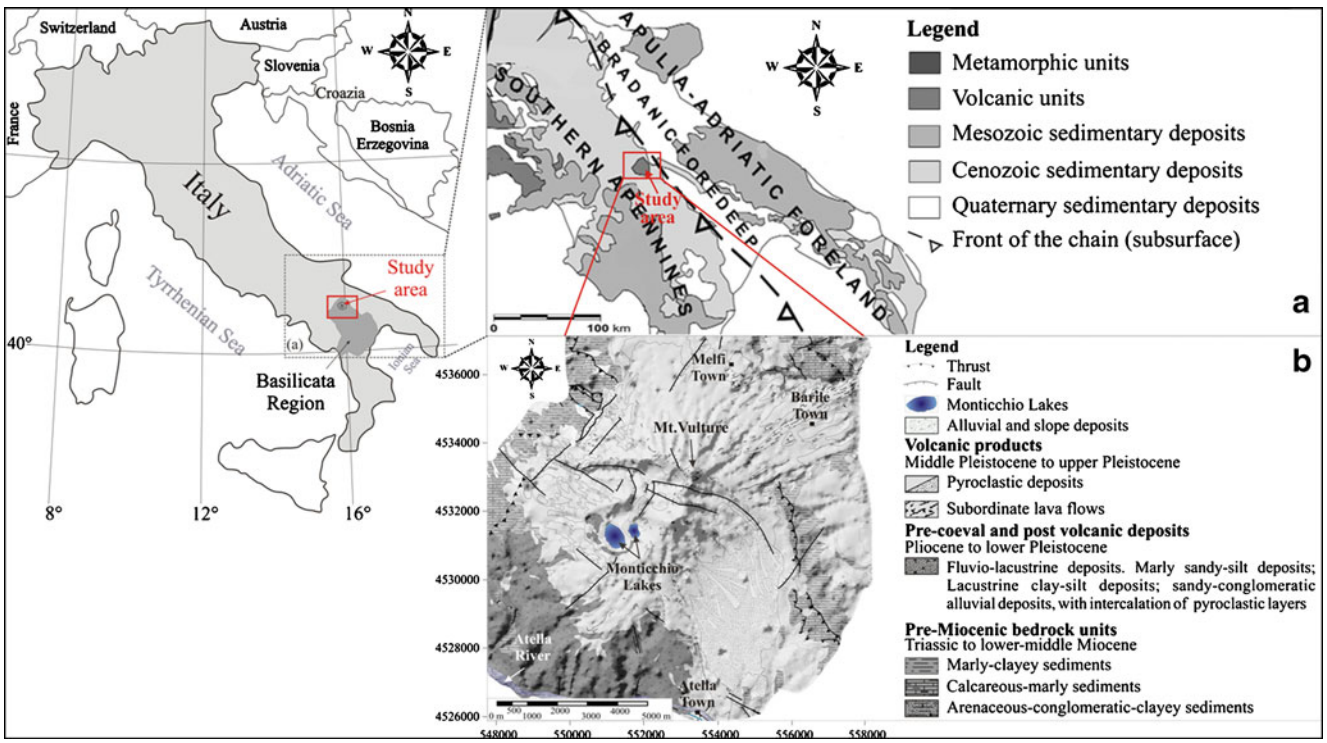

Fig. 1 **a** Geological map of central-southern Italy (from Bonardi et al. 2009, modified). **b** Geological setting of Mt. Vulture area (base geological map by Giannandrea et al. 2004, modified). The geological map is provided in Italian Gauss-Boaga, Zone Est coordinates, using the Roma Datum of 1940

 DOI 10.1007/s10040-010-0619-8

oldest pre-Miocene bedrock units consist principally of deep-sea sediments belonging to units ranging from early Triassic to lower-middle Miocene (Boenzi et al. 1987; Principe and Giannandrea 2002). Beneath the Meso-Cenozoic substratum units, radiolarians and limestones of the Apulian platform are found to a depth of about 5 km (La Volpe et al. 1984). The fracture-fault systems characterized by NW–SE, NNW–SSE and E–W normal faults (Beneduce and Giano 1996; Schiattarella et al. 2005) involve the Mt. Vulture volcanic products and the bedrock units as well, highlighting a concentric-radial pattern jointed to the volcanic events, which controlled the area drainage system evolution, principally oriented in NW–SE and E–W directions (Ciccacci et al. 1999).

Climate

According to UNESCO/FAO (1963), the study area has a temperate Mediterranean climate, with moderately hot summers and cold winters. It shows a mean annual rainfall of about 750 mm year^{-1} (data based on observations from 1964 to 2006, Hydrographic Service of Civil Engineers of Puglia Region) with a maximum amount of rainfall from November to January (Fig. 2a). The maximum rainfall amounts are associated with the highest elevations of the study area (Fig. 2a). Spilotro et al. (2000) estimated an average annual precipitation of about 850–650 mm year^{-1} and a potential evapotranspiration of about 580 mm year^{-1}. The annual average temperature for the Vulture area is about 13°C (data from 1964 to 2006), with a maximum from June to August (22°C) and a minimum between December and February (~5°C) (Fig. 2b).

Hydrogeology

The Mt. Vulture basin represents one of the most important aquifer systems of southern Italy. The aquifer core is mainly constituted of pyroclastic and subordinate lava flow layers, with different permeabilities which locally give rise to distinct aquifer layers. The principal hydrogeological complexes are volcanic products, with high-medium permeability values composed mainly of pyroclastic deposits and subordinate lava flows, which are the principal host aquifer rocks, of the Mt. Vulture basin (Fig. 3). The porous and fractured lava flows show a hydraulic conductivity (K) of about 10^{-1} cm s^{-1}, while in the tuff and the incoherent pyroclastic deposits, with intergranular porosity, K is less ($\approx 10^{-3}$ cm s^{-1}). In the fluvio-lacustrine gravel deposits of the Fiumara di Atella Super-synthems, K is $\approx 10^{-2}$ cm s^{-1} (Spilotro et al. 2005). The structural hydraulic parameters and anisotropy features of the aquifer are the major factors that control groundwater flow pathways. Toward the S–SE, the volcanic aquifer thickness decreases considerably, leading to groundwater discharge where Fiumara di Atella Super-synthems deposits constitute a local extension of the volcanic aquifer with a relatively low groundwater circulation. Flow direction and rates are controlled primarily by the properties of the rock matrix and secondarily by the existing fracture network. The bedrock units are the marly-clayey complex, the calcareous-marly complex and arenaceous-conglomeratic-clayey complex showing less permeability. The different permeabilities of the volcanic products, fluvio-lacustrine deposits and the sedimentary bedrock allowed the construction of a detailed hydrogeological map (Fig. 3). The permeability of the aquifer host rocks varies from the highest to the lowest elevations of the Mt. Vulture basin. The juxtaposition of these hydrogeological features leads to different groundwater flowpaths and helps to better identify the main processes affecting the geochemistry of the groundwaters.

Two conceptual hydrogeological models have been proposed for the Mt. Vulture aquifer. Celico and Summa (2004) hypothesize two independent hydrogeological basins—one in the S–SE Monticchio-Atella sector, and one in the northeast Melfi-Barile area. The proposed southeastern groundwater basin is located between the most important faults of the volcano: the Grigi Valley-Fosso del Corbo fault to the north, and an unnamed fault in the south (Schiattarella et al. 2005). The proposed northeastern basin is the Melfi-Barile, characterized by radial drainage. The presence or absence of permeable rocks locally determines the existence of more inter-communicating basal layers. Recently Spilotro et al. (2005, 2006) suggested a new conceptual hydrogeological model in which the Mt. Vulture volcanic edifice is a huge aquifer where the spring regime shows a slightly seasonal variation of flow. As suggested by Spilotro et al. (2006), the surface drainage network constitutes the natural limits of the water catchments, where the pseudo-tectonic structure of Grigi Valley–Fosso del Corbo Fault is the only drainage axis widely affecting preferential groundwater flow and no evidence for the presence of the southern fault as a subordinate drainage axis was observed. The permeability and anisotropy features of the volcanic aquifer are the result of the magmatic and pyroclastic sequences and their successive arrangement and tectonic-volcanogenic deformation, creating locally shallower groundwater flows (Spilotro et al. 2006). As identified by Spilotro et al. (2006), the spring regime shows a slightly seasonal variation of flow, with higher values in spring and lower values in autumn.

Although different conceptual models of the Mt Vulture basin have been developed, they are mostly based on hydrochemical, hydraulic and geological observations. This study demonstrates how far the use of environmental tracers and their application to determine recharge sources and elevations of groundwater provide an efficient tool to improve the current understanding of hydrogeological systems.

Methodology, sampling and analytical procedures

This study reports analytical data for 48 groundwater sources (Fig. 3), located at elevations ranging from 352 to 1,000 m a.s.l., and including drilled wells used for

 DOI 10.1007/s10040-010-0619-8

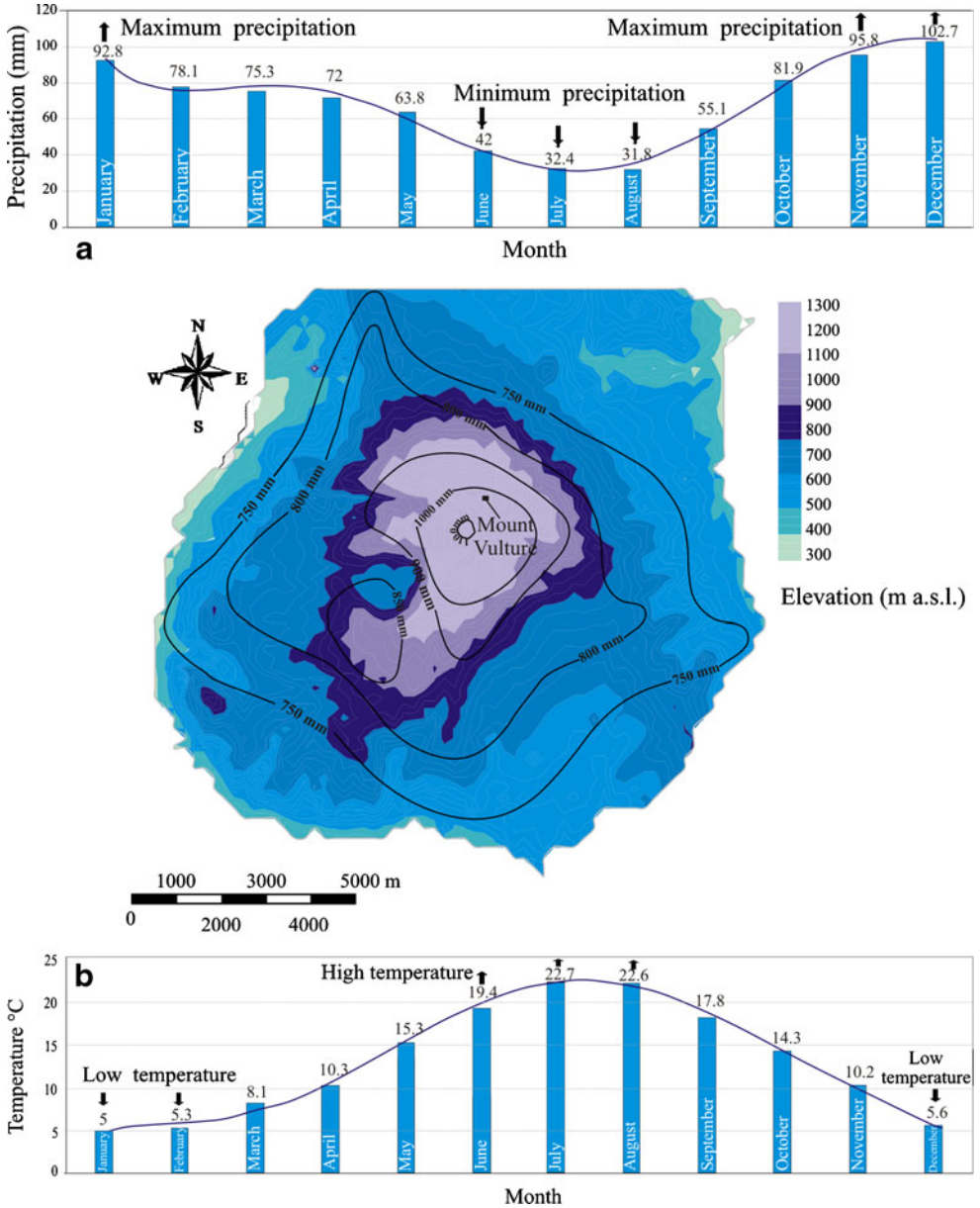

Fig. 2 **a** Mean monthly precipitation based on 40 years of observation (data from Hydrographic Service of Civil Engineers of Puglia Region, measured at Melfi gauge station, elevation 580 m a.s.l.). The *upward arrows* indicate the months characterized by maximum precipitation amount; while the *downward arrows* indicate the months characterized by minimum precipitation amount. The map shows the yearly rainfall distribution (contours) over the study area (data from Hydrographic Service of Civil Engineers of Puglia Region) in relation to topographic elevation. **b** Mean monthly temperature for 40 years of observation (data from Hydrographic Service of Civil Engineers of Puglia Region, measured at Melfi gauge station, elevation 580 m a.s.l.). The *upward arrows* indicate the months characterized by highest temperatures, while the *downward arrows* indicate the months characterized by lowest temperature

irrigation and drinking-water supply and some springs. Sampling sites are located mainly in the W–NW, S–SE and N–NE sectors of the study area, principally within the volcanic units. Some sampling points of the S–SE and N–NE sectors are located within the fluvio-lacustrine sediments from Pliocene to lower Pleistocene age. Details of the sampling points are given in Table 1 (all location data are provided in UTM Zone 33 coordinates, using the European Datum of 1950). Seventeen sampled springs are characterized by elevation ranging from 352 to 960 m a.s.l. Thirty-one groundwaters samples were taken from the operating vertical and horizontal wells of several companies and private owners. The well depth and/or length is between 22 and 220 m and many of them are constructed inside the volcanic units (pyroclastic and effusive rocks).

A complete hydraulic dataset of the inventory performed by Regione Basilicata (1987, 1989; elevation of water levels in public/private wells and springs) has been integrated with measurements carried out in the present study using a global positioning system instrument (5-m precision) and piezometric level sensor (LP10) with high accuracy.

 DOI 10.1007/s10040-010-0619-8

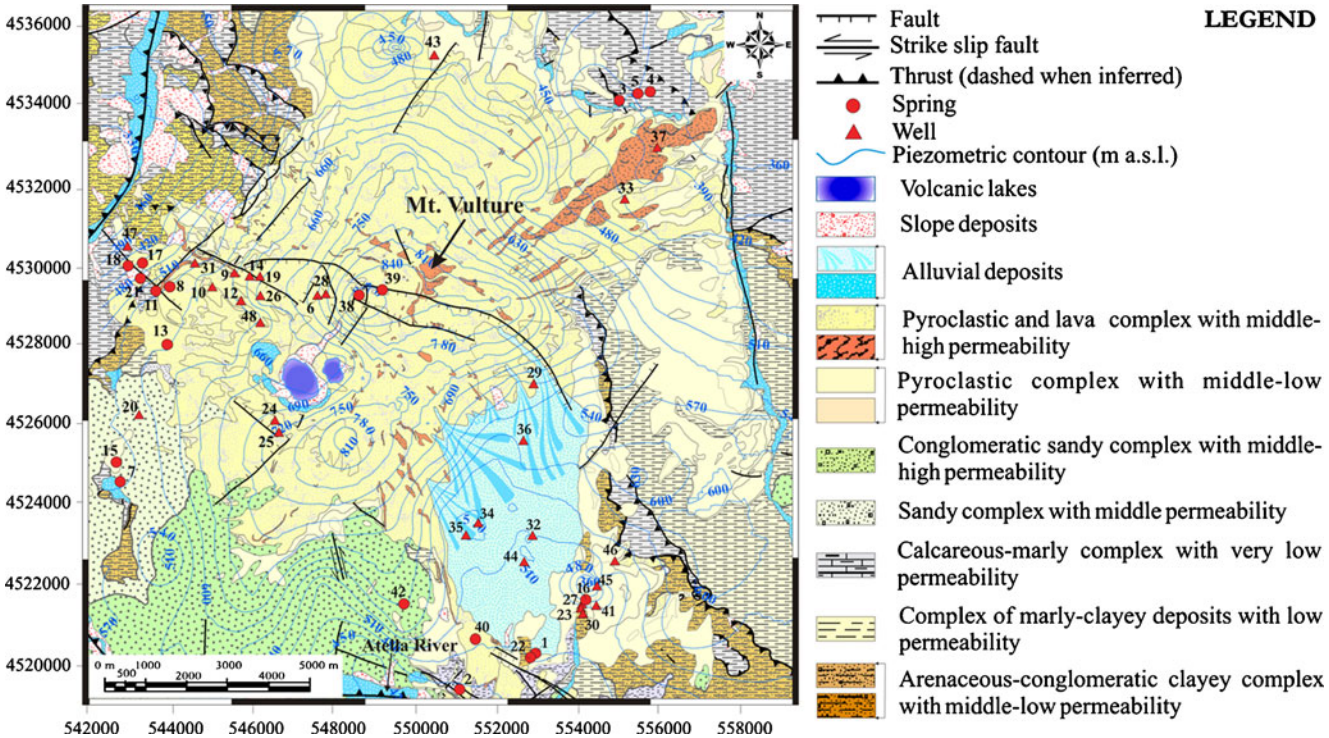

Fig. 3 Hydrogeological map of the Mt. Vulture basin showing the main hydrogeological complexes (by Spilotro et al. 2006; modified) and the sampling points used for this study. The contour interval for the piezometric surface is 30 m. The map and the location data are provided in UTM Zone 33 coordinates, using the European Datum of 1950. Geology base map by Giannandrea et al. (2004)

The water samples were collected during three sampling campaigns, from June 2007 to June 2008, for stable isotopes (^{18}O, D) and major constituents (Ca^{2+}, Mg^{2+}, Na^{+}, K^{+}, Cl^{-}, SO_4^{2-}, NO_3^{-}).

Measurements for water pH, temperature, electrical conductivity (EC), Eh and discharge were determined with high-resolution multiparametric probes (Idronaut, Ocean Seven 305; WTW–Tetracon 325). All water samples were stored in high-density polyethylene (HDPE; 50 ml) bottles with watertight caps, after filtration through a 0.45 μm Millipore filter for cation and anion analysis. Samples for cation analysis were preserved by acidifying to pH ~2 with concentrated HNO_3. Alkalinity was determined in the field by titration with HCl (0.1 M). After sampling, all samples were stored at 4°C. Major ion determinations were carried out in the Gaudianello Spa laboratory on unacidified (F^{-}, Cl^{-}, $NO_3^{-}$and SO_4^{2-}) and acidified (Na^{+}, K^{+}, Ca^{2+}, Mg^{2+}) water samples with separate aliquots by ion chromatography (Dionex CX-100). Ionic balance was computed for each sample taking into account major species. All samples exhibited imbalances lower than 5%.

The isotope investigations (δD and $\delta^{18}O$) were carried out for 48 groundwater locations, at which samples were collected one to three times during the present survey. Water samples were also analyzed at the Alfred Wegener Institute in Potsdam using a common equilibration technique with a Finnigan MAT Delta-S mass spectrometer equipped with two equilibration units for the online determination of hydrogen and oxygen isotopic composition (Meyer et al. 2000). The isotopic composition is based on international reference materials, V-SMOW (Vienna Standard Mean Ocean Water), as standard. The external errors of long-term standard measurements for hydrogen and oxygen are better than 0.8 and 0.1‰, respectively. Stable isotope compositions are reported, hereafter, as δ-values in parts per thousand (‰), calculated with respect to the V-SMOW international standard. The δ values are given by:

$$\delta(‰) = 1000‰ \cdot \left(\frac{R_{\text{sample}} - R_{\text{V-SMOW}}}{R_{\text{V-SMOW}}} \right)$$

where R_{sample} and $R_{\text{V-SMOW}}$ represent the ratios of heavier to lighter isotopes ($^2H/^1H$ or $^{18}O/^{16}O$). R_{sample} and $R_{\text{V-SMOW}}$ are the isotope ratios in the sample and the standard respectively. The sample is described as depleted in the heavier isotopes if the δ values are lower (more negative), and in contrast it is enriched in the heavier isotopes if the δ values are higher (more positive).

Results

Groundwater flowpaths

The existing groundwater flow information comes from water discharge points, including 106 springs and 119 shallow and deep wells (data from census of Regione Basilicata 1987, 1989,) consisting of unpublished static water level data from private wells (Gaudianello SpA; Traficante Srl, Itala Srl, Cutolo Srl) and public wells (Consortium of Melfi, National Irrigation Corporation)

 DOI 10.1007/s10040-010-0619-8

Table 1 Description of sample collection sites. All location data are provided in UTM Zone 33 coordinates, using the European Datum of 1950. Elevation in m a.s.l. (meters above sea level); *NA* not available; *well depth* depth (meters) for vertical wells; *well length* length (meters) for horizontal wells

No.	Station name	Type	Locality	Elevation (m a.s.l)	Long. (North)	Lat. (East)	Well depth (m)	Well length	Discharge ($L\ s^{-1}$)
1	Atella F1	Spring	Atella town	461	4525900	555400	-	-	0.01
2	Atella F3	Spring	Atella town	394	4524880	554180	-	-	<0.01
3	Rapolla 2	Spring	Rapolla town	360	4536654	557111	-	-	0.14
4	Rapolla 1	Spring	Rapolla town	352	4536649	557081	-	-	0.13
5	Acetosella	Spring	Rupe di Gallo	365	4536694	557091	-	-	0.14
6	Pozzo 22 V	Vertical well	Gaudianello SpA Company	690	4532938	551154	157.5		2.5
7	S.Maria de Luco 2	Spring	Monticchio Sgarroni	519	4529475	547254	-	-	<0.01
8	Eudria 5	Spring	C.da 5 Cerri	551	4533080	548200	-	-	0.10
9	Sorgente 34 bis	Horizontal well	Gaudianello SpA Company	657	4533379	549532		643	1.5
10	Gaudio 11 V	Vertical well	Gaudianello SpA Company	644	4533100	549100	202		0.70
11	Eudria 2	Vertical well	C.da 5 Cerri	547	4532983	547976	-	-	<0.01
12	Pozzo 20 V	Vertical well	Gaudianello SpA Company	650	4532832	549658	96		5
13	Crocco	Spring	Piana Ferriera	575	4531940	548200	-	-	0.13
14	Sorgente 35	Horizontal well	Gaudianello SpA Company	566	4533314	549828		183	0.97
15	S.Maria de Luco 1	Spring	Monticchio Sgarroni	515	4529640	547200	-	-	<0.01
16	Nettuno	Horizontal well	Itala Company	487	4526955	556359		130	9
17	Eudria 3	Spring	C.da 5 Cerri	558	4533536	547715	-	-	0.43
18	Eudria 4	Spring	C.da 5 Cerri	554	4533481	547438	-	-	0.11
19	Sorgente 36	Horizontal well	Gaudianello SpA Company	565	4533306	550031	-	208	0.49
20	Pozzo 23 V	Vertical well	Gaudianello SpA Company	682	4530603	547666	144		2.5
21	Eudria 1	Spring	C.da 5 Cerri	547	4533230	547678	-	-	<0.01
22	Atella 2	Spring	Atella town	474	4525820	555300	-	-	0.05
23	Fonte Itala 1	Vertical well	Itala Company	490	4526900	556320	NA		1.5
24	Giovanna	Vertical well	Mont. Sgarroni-Rionero	813	4530492	550326	75		3.5
25	Angelicchio	Vertical well	Mont. Sgarroni-Rionero	820	4530260	550400	75		2.5
26	Gaudio 21 V	Vertical well	Gaudianello SpA Company	735	4532930	550040	202		6
27	Fonte Itala 2	Horizontal well	Itala Company	490	4526817	556303		n.a	4.3
28	Pozzo 24 V	Vertical well	Gaudianello SpA Company	780	4532966	551315	251		2.5
29	Pozzo 4	Vertical well	C.da Gaudio	545	4531210	555380	150		<0.01
30	San Marco	Horizontal well	Itala Company	490	4526707	556342		n.a	2.5
31	Pozzo 15 V	Vertical well	Gaudianello SpA Company	555	4533672	548815	44		8
32	Pozzo 3	Vertical well	C.da Gaudio	545	4528240	555360	127.5		0.42
33	Pozzo D	Vertical well	Piana della Cicoria	519	4534820	557160	133		13
34	Pozzo 5	Vertical well	Monastero S. Maria degli	544	4528490	554302	96.5		<0.01
35	Pozzo A	Vertical well	Piana del Gaudio	600	4528250	554060	132		0.11
36	Pozzo B	Vertical well	Piana del Gaudio	626	4530101	555179	150		<0.01
37	Pozzo 2	Vertical well	Ciaulino	686	4535826	557800	78		15
38	Fontana dei Faggi	Spring	Foresta di Monticchio	885	4532900	551950	-	-	0.23
39	Piloni	Spring	Valle dei Melaggini	960	4533066	552194	-	-	<0.01
40	Fonte Tripoli	Spring	La Franesca	488	4526177	554225	-	-	2
41	Pozzo Dilva	Vertical well	La Franesca	493	4526870	556607	60		5
42	Sorgente Bosco Bufara	Spring	Bosco della Bufata	449	4526867	552828	-	-	0.11
43	Savino	Vertical well	Melfi	535	4537640	553440	101		10
44	Sveva 2	Vertical well	La Franesca	554	4527726	555196	250		9.5
45	Sveva	Vertical well	La Franesca	517	4527260	556620	180		2.7
46	Lilia 2	Vertical well	Piana del Gaudio	552	4527739	556970	132		6.7
47	Toka	Vertical well	Monticchio Bagni	396	4533900	547440	22		3.5
48	Solaria	Vertical well	Monticchio Bagni	643	4532408	550040	110		2.2

and the distribution of springs and their elevations. No significant groundwater level changes were observed when comparing the three samplings, from June 2007 to June 2008, confirming the suggestion of Spilotro et al. (2005) that the levels are fairly consistent.

A piezometric-surface map has been drawn using the geostatistical method of 'ordinary kriging' using SURFER software (Golden Software). As shown in Figs. 4 and 5, groundwater flowing within the volcanic aquifer moves from the highest to the lowest elevations along radial streamlines, illustrated by the flow arrows that are perpendicular to the lines of constant head. However, in some limited areas the different slope of the flow arrows is due to the automatic interpolation of the ordinary kriging geostatistical methods which do not show the real situation.

The radial deposition of the volcanic products favors groundwater flow from the highest elevations towards the periphery areas, as proposed by Spilotro et al. (2006). The irregularities in the radial symmetry of the aquifer are indicated by the equipotential lines. In the NW and SE sectors, these differences are probably due to the presence of the most important pseudo-tectonic structure (Grigi Valley–Fosso del Corbo Fault) with a NE–SE trend; while

 DOI 10.1007/s10040-010-0619-8

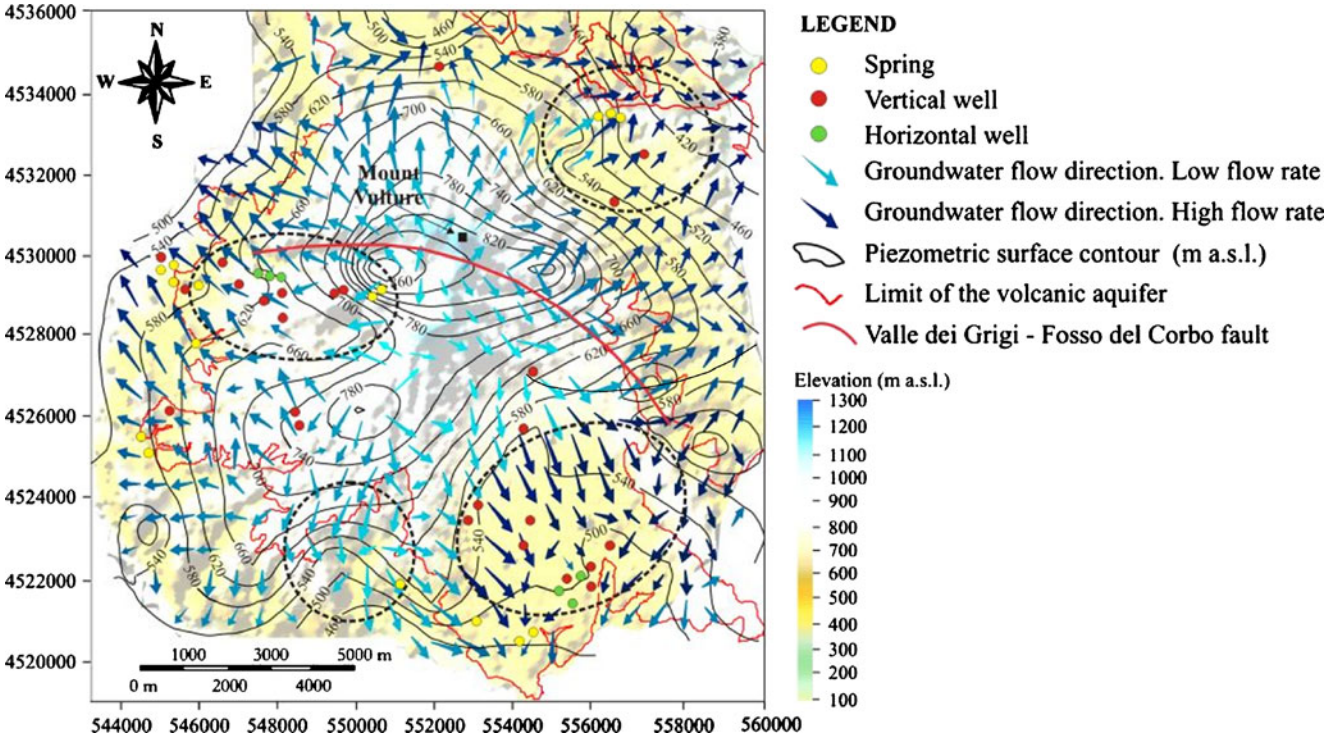

Fig. 4 Water-table map, obtained using ordinary kriging (SURFER software, Golden Software), shows the irregularities of the piezometric surface. The *circles drawn with black dotted lines* encompass the irregularities of the constant head contour lines. The Grigi Valley–Fosso del Corbo Fault is shown as a *red line*. The map and the location data are provided in UTM Zone 33 coordinates, using the European Datum of 1950. The contour interval used for the piezometric surface is 40 m. The *arrows* show the groundwater flowpaths

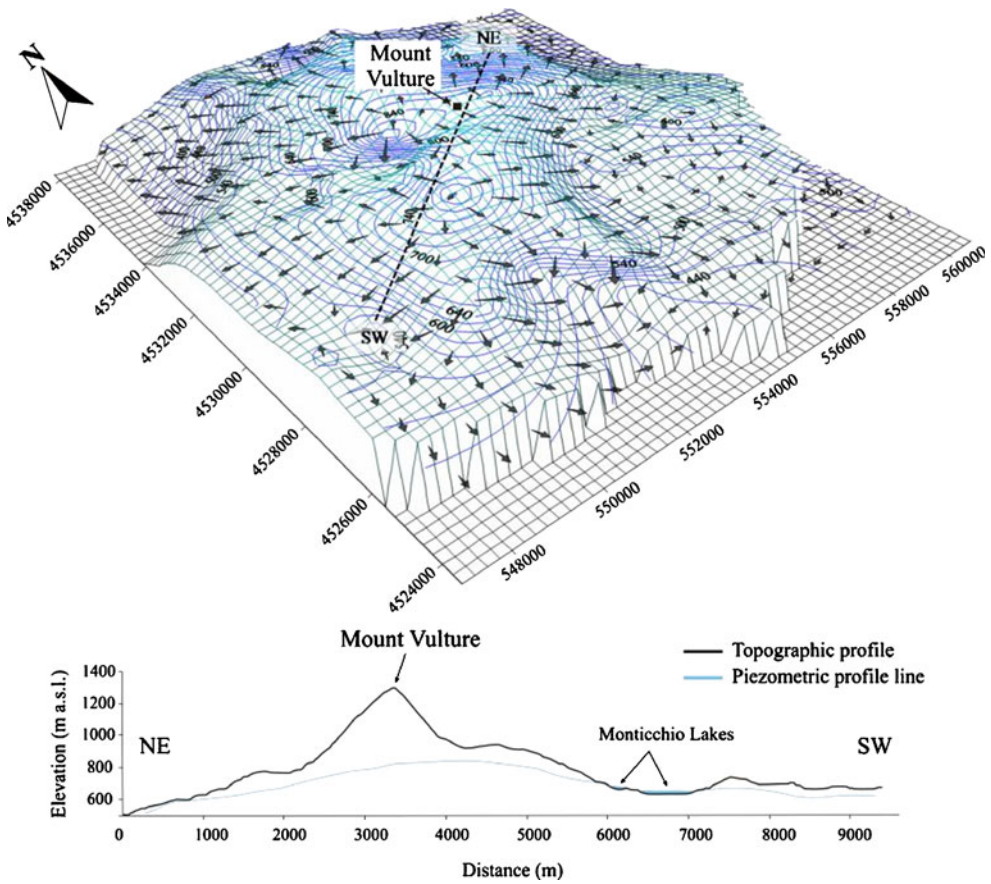

Fig. 5 Piezometric elevation map showing the piezometric surface gradients (using SURFER). All the location data are provided in UTM Zone 33 coordinates, using the European Datum of 1950

 DOI 10.1007/s10040-010-0619-8

in the orthogonal directions the presence of lower permeability hydrogeological complexes lead to minor changes in the piezometric surface (Fig. 4).

The map/graph of the piezometric profile line of the volcanic aquifer shows that there are quite steep vertical groundwater gradients (Fig. 5). The present hydrogeological and hydraulic studies give emphasis to the conceptual hydrogeological model proposed by Spilotro et al. (2006). The isotopic investigation discussed in the following contributes additional knowledge of the Mt. Vulture volcanic aquifer.

Groundwater–chemical composition

The ionic compositions of the analyzed water samples are reported in Table 2. Observed groundwater temperatures range from 10°C (cold water) to 19.8°C (slightly thermal waters). 'Thermal water' is a term that was introduced by Nathenson et al. (2003) for springs which do not meet the numerical criterion of Reed (1983) but have temperature higher than non-thermal springs and usually have also dissolved constituents normally found in thermal waters. At the mean and low elevations, the temperatures of the groundwater (mean values 16.3°C) following the shallow flowpaths, were slightly above the mean annual air temperature (13.5°C).

The analyzed shallow and deep groundwater samples have variable pH values and redox state (Eh) which range from slightly acidic to neutral (pH 5.4–7.5) and from slightly reduced to oxidized (–36 mV< Eh< +185 mV), respectively; probably reflecting differences in circulation paths, water discharge and residence times within the aquifer. The increase in water acidity is principally due to the dissolution of CO_2, which is the principal gas of magmatic origin. The high-dissolved CO_2 contents in the groundwater of the volcanic aquifer are probably due to the ongoing active magmatic-mantle outgassing (Caracausi et al. 2009; Paternoster 2005). The mean EC values vary between 0.19and 17.97 ms cm^{-1}. From the 1980s until 2006, the value of the EC increased more than 15% (data from census of Regione Basilicata 1987, 1989), probably due to decreases in total annual precipitation. The mean TDS values of the individual sites range from 208 to 18,000 mg L^{-1}.

As shown in the Stiff and Piper diagrams (Fig. 6), the Vulture groundwaters generally display a chemical composition from bicarbonate alkaline-earth (group 1) to sulphate-bicarbonate alkaline (group 2). The principal dissolved anion bicarbonate is resulting from the reaction of dissolved CO_2 to form HCO_3 (Stumm and Morgan 1996). In contrast to soil CO_2 in the unsaturated zone, the deep CO_2 is directly injected in the saturated zone, with a high initial CO_2 content, and therefore a low initial pH value. The low-pH water is very aggressive towards the host volcanic rocks, leaching their more soluble components. As a consequence, major ion constituents are progressively brought into solution, pH increases to the typical values measured in Vulture groundwaters, and CO_2 is partially converted to bicarbonate. The dissolution of the host rocks depends on contact time between the rocks and water. Deep CO_2 produces a fast and extensive enlargement of the fracture systems in the host rocks principally in the saturated zone and it may create a specific organization of flow patterns in the saturated zone (Annunziatellis et al. 2008 and references therein).

Most of the water samples show high concentrations of Na^+, K^+, and Ca^{2+}. The Na-excess found in a few analyzed water samples may be due to the hydrolysis of Na-silicates and also due to the exchange of Ca^{2+} for Na^+, on the surfaces of clay-minerals (Na-smectite). This indicates an intensive water–rock interaction process, in agreement with results of Paternoster et al. (2009).

A few springs with the highest TDS values and a sulphate-bicarbonate alkaline composition showed higher mineralization, with elevated contents of SO_4^{2-}, Na^+, Cl^-, and dissolved CO_2. As reported by Paternoster et al. (2009), the $\delta^{34}S$ (SO_4^{2-}) isotopic compositions of groundwaters with the highest concentration of SO_4^{2-}, displays sulphur isotopic values similar to those measured by Marini et al. (1994) in the magmas, supporting a main origin from the leaching of mineral weathering products such as feldspathoids, belonging to the sodalite group found in the volcanic host rocks. This similarity of sulphur isotopic values is due to the longer residence times of groundwater within the host rocks, representing the local extension of the volcanic aquifer where fluvio-lacustrine sediments with intercalated pyroclastic layers could contain entrapped brackish groundwaters. Along the flow path, from the mountainous area to the lower elevations close to the Atella River (Fig. 1), which drains the south part of the Vulture area, the groundwaters have the highest content of dissolved ions (Fig. 6a). In the W–NW sector, the groundwaters are characterized by lower mineralization values showing a bicarbonate alkaline-earth composition as a consequence of the interaction between volcanic rocks and groundwaters of meteoric origin, flowing at high-mid elevations, characterized by flowpaths with shorter residence times. At the lower elevations in the S–SE sectors, the springs near the base of the aquifer and occasionally in contact with the fluvio-lacustrine deposits, with intercalations of pyroclastic layers, are characterized as sulphate-bicarbonate alkaline composition with high salinity. This hydrogeochemistry variation is due to the deeper and lengthy flow pathways with longer groundwater residence time.

The hydrogeochemical differences between waters at the highest elevations, which probably are the main recharge areas, and the samples taken at the lowest elevations are consistent with the conceptual hydrogeological model previously described, from the core to the boundaries of the aquifer, indicating an important role played by aquifer radial symmetry.

Stable isotopic analysis ($\delta^{18}O$ and δD)

Comparison of the stable isotopic compositions of precipitation and groundwater provides an excellent tool for evaluating recharge areas (Clark and Fritz 1997; Jones and Banner 2003). The principal groundwater recharge areas of the Mt. Vulture basin are identified using the

 DOI 10.1007/s10040-010-0619-8

Table 2 Dissolved contents of groundwater. Temperature, EC, pH, and Eh were measured in situ with a multiparametric probe that provided values assuming a water temperature of 20°C. The values reported are the arithmetic means of three samplings; *BDL* below detection limit; *NM* not measured

No.	Station Name	Field pH	Field EC	Field Eh	Field Temp.	Li^+	Na^+	K^+	Mg^{2+}	Ca^{2+}	F^-	Cl^-	NO_3^-	SO_4^{2-}	Field HCO_3^-	SiO_2	TDS	Charge balance error
			(mS cm^{-1})	mV	°C	(mg L^{-1})												(%)
1	Atella F1	6.8	17.97	–27	16.3	1.90	4,190	875	142	175	1.4	1,160	40	4,970	6,128	29	17,712	–4.9
2	Atella F3	6.4	11.7	16	17.1	3.41	3,652	416	97	241	1.1	1,080	56	4,110	3,892	33	13,580	4.9
3	Rapolla 2	6.5	7.66	11	16.3	1.49	2,363	150	27	177	1.0	820.0	39	2,710	2,147	89	8,525	2.1
4	Rapolla 1	6.1	4.13	37	16.5	0.78	1,170	93	17	96	1.4	350	30	1,097	1,452	70	4,377	4.3
5	Acetosella	6.3	2.59	24	16.8	0.64	1,080	76	14	64	1.3	240	16	770	1,721	80	4,063	3.8
6	Pozzo 22 V	5.9	2.59	NM	19.1	0.09	145	57	59	89	0.3	33	1.7	74	841	106	1,406	4.7
7	S.Maria de Luco 2	5.9	2.15	48	15.1	0.05	132	20	17	169	0.2	54	36	73	715	31	1,247	4.7
8	Eudria 5	5.9	1.89	50	17.3	0.09	169	57	74	45	0.4	48	10	145	792	99	1,442	–2.1
9	Sorgente 34 bis	6.1	1.84	NM	15.1	0.01	41	22	11	33	0.5	26	2	41	209	108	493	–4.2
10	Gaudio 11 V	5.8	1.77	NM	19	0.07	144	39	47	117	0.5	38	12	87	911	97	1,492	–4.7
11	Eudria 2	6.0	2.64	39	19.4	0.17	312	68	117	114	0.3	46	3.6	205	1,435	111	2,412	4.9
12	Pozzo 20 V	5.9	1.45	NM	19.8	0.11	184	56	75	48	0.3	41	1.1	170	780	110	1,465	2.8
13	Crocco	5.9	1.33	51	16.6	0.11	125	38	52	130	0.4	34	0.3	130	794	107	1,410	2.6
14	Sorgente 35	5.7	1.33	NM	17.2	0.08	93	33	35	105	0.5	35	3.4	99	568	104	1,076	4.4
15	S.Maria de Luco 1	6.1	1.27	33	14.8	0.03	62	12	12	51	0.3	44	42	40	252	31	546	–4.9
16	Nettuno	5.8	1.15	NM	15.5	0.12	148	47	31	135.2	1.1	28	18	75	825	95	1,402	4.5
17	Eudria 3	5.6	1.57	63	16.5	0.06	76	28	42	136	0.6	64	94	86	515	104	1,146	4.8
18	Eudria 4	5.4	1.15	–31	15.3	0.07	128	41	61	135	0.4	42	20	117	828	109	1,481	4.6
19	Sorgente 36	5.9	0.97	NM	18.2	0.09	173	55	74	83	0.5	36	2.4	154	964	97	1,639	–4.9
20	Pozzo 23 V	5.9	0.9	NM	19	0.05	74	39	35	95	0.5	31	2.1	39	609	106	1,030	0.9
21	Eudria 1	5.5	0.89	69	15.9	0.06	72	31	33	101	0.6	26	8.2	41	585	100	998	3.4
22	Atella 2	5.8	0.88	62	15.2	0.08	97	26	16	91	1.2	32	11	92	451	83	899	2.5
23	Fonte Itala 1	5.9	0.73	NM	17.6	0.06	80	32	15	62	1.1	19	15	44	443	100	811	–3.8
24	Giovanna	7.3	0.7	–31	13	BDL	30	22	14	78	0.6	13	37	23	341	49	608	–1.8
25	Angelicchio	7.5	0.68	–36	13.6	BDL	39	16	19	75	0.6	30	83	21	307	52	642	–4.2
26	Gaudio 21 V	5.9	0.53	NM	15.9	0.03	54	32	13	53	0.5	25	12	14	338	112	653	4.9
27	Fonte Itala 2	5.9	0.51	NM	15.8	0.05	56	19	10	38	1.5	14	35	20	258	86	538	–0.1
28	Pozzo 24 V	5.8	0.46	NM	16	0.02	42	29	10	33	0.5	26	9	11	250	107	518	–3.4
29	Pozzo 4	5.6	0.44	185	14	0.02	35	16	11	36	0.5	31	40	16	180	77	443	–4.3
30	San Marco	5.8	0.42	NM	15.9	0.03	39	17	18	57	0.5	16	29	13	340	92	621	–4.8
31	Pozzo 15 V	5.9	0.41	NM	19.6	0.19	258	57	94	106	0.5	44	3.2	188	1,178	103	2,031	4.9
32	Pozzo 3	6.3	0.39	38	13.5	0.01	125	16	13	53	0.6	15	26	9	543	82	882	–4.2
33	Pozzo D	6.5	0.32	24	16.1	BDL	38	16	7	45	0.3	18	17	15	237	81	475	–1.7
34	Pozzo 5	7.0	0.29	–13	15.6	0.03	27	17	5	23	1.4	12	28	9	136	82	341	–1.6
35	Pozzo A	7.1	0.29	–14	15.7	BDL	27	13	7	35	0.9	13	28	8	176	71	377	3.1
36	Pozzo B	6.3	0.29	38	15.7	BDL	32	23	BDL	18	0.7	13	21	7	148	85	347	–1.2
37	Pozzo 2	5.8	0.28	67	14.8	BDL	31	20	5	23	0.3	15	14	8	147	97	360	4.1
38	Fontana dei Faggi	6.7	0.26	15	10	BDL	16	9	6	33	0.6	21	2.8	10	122	50	269	4.1
39	Piloni	7.4	0.19	–29	10.3	BDL	14	7	5	22	0.3	19	3.7	15	89	42	217	–4.3
40	Fonte Tripoli	5.8	0.74	64	15.3	BDL	14	3	BDL	12	0.2	7	3.3	9	55	104	208	–2.8
41	Pozzo Dilva	6.4	0.31	29	14.6	BDL	28	19	8	55	0.7	11	25	12	202	38	399	–4.0
42	Sorgente Bosco della Bufara	6.4	4.71	29	15.8	0.67	491	112	45	75	0.2	188	2.9	660	871	67	2,512	–4.8
43	Savino	7.2	0.84	–24	16.5	0.07	112	32	8	34	1.5	37	0.5	102	319	70	718	–4.3
44	Sveva 2	6.1	2.1	40	19	0.3	267	63	43	201	1.2	28	0.3	110	1,488	88	2,291	–2.6
45	Sveva	6.2	0.96	36	15.6	0.07	157	20	13	70	0.9	37	18	125	463	83	986	2.9
46	Lilia 2	6.1	0.45	40	16.7	0.08	56	26	9	58	1.1	16	8.9	11	338	97	621	4.6
47	Toka	6.4	0.54	24	15.7	0.13	405	101	54	167	0.8	95	31	355	1,284	64	2,556	0.9
48	Solaria	6.2	2.81	33	16.1	0.12	52	24	19	86	1.1	33	6.5	60	291	83	655	–4.7

yearly mean isotopic composition of water from precipitation samples collected monthly over a 2-year period by Paternoster et al. (2008). Using five rain gauges, elevations ranging from 320 to 1285 m a.s.l., the local meteoric water line (LMWL) and the weighted local meteoric water line (WLMWL) were defined. The rainwater isotopic composition showed a wide range of variation from –12.2 to –2.9‰ for $\delta^{18}O$ and from –79 to –19‰ for δD, due to seasonal and elevation effects, but sometimes one effect prevails over another.

 DOI 10.1007/s10040-010-0619-8

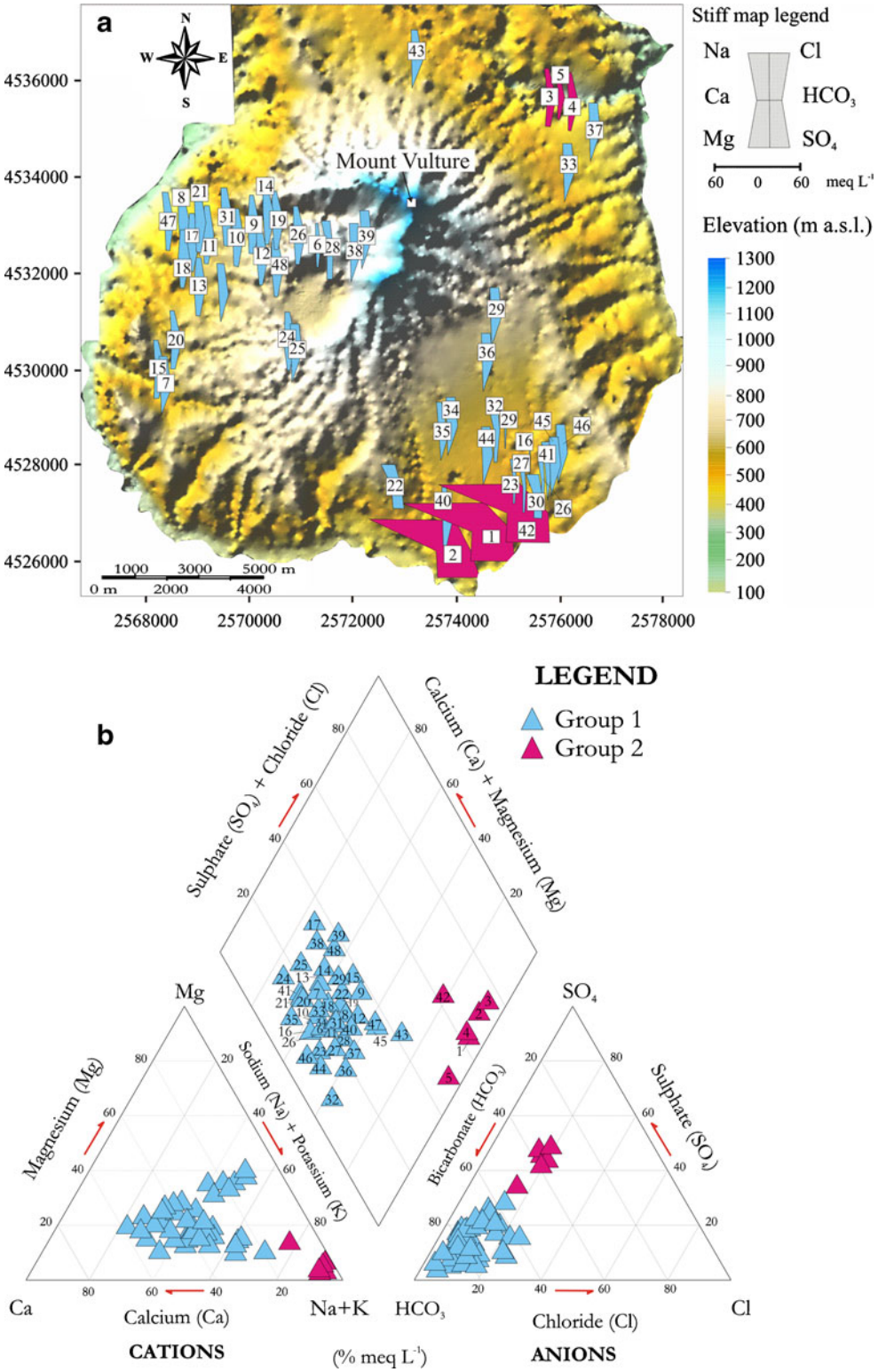

Fig. 6 Relative amounts of major ions analyzed in springs and wells, plotted with **a** Stiff diagrams on the map, and **b** a Piper plot. All the location data are provided in UTM Zone 33 coordinates, using the European Datum of 1950

Stable isotopic composition of precipitation: seasonal and elevation effects

Dansgaard (1964) recognized the inverse correlation between the $\delta^{18}O$ and δD of precipitation with temperature. With respect to the seasonal effect, Fig. 7 shows that the precipitation in summer months, when the air temperature values are higher, is characterized by heavier isotopic composition. On the other hand, winter precipitation has lighter isotopic composition.

 DOI 10.1007/s10040-010-0619-8

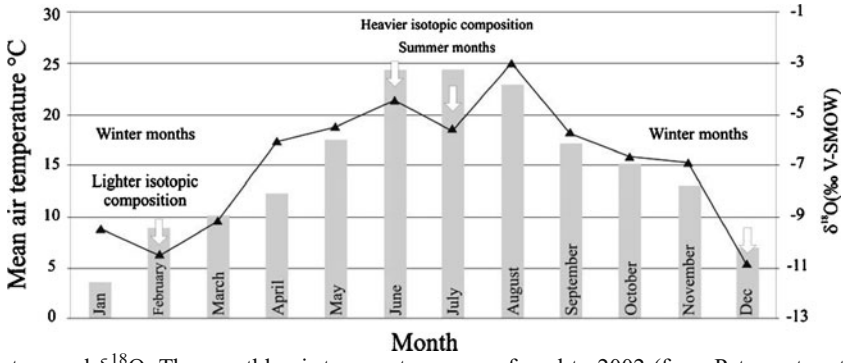

Fig. 7 Mean air temperature and $\delta^{18}O$. The monthly air temperatures are referred to 2002 (from Paternoster et al. 2008). The *grey bars* represent the mean air temperature and the *black and blue line/circles* represent the isotopic composition. The *arrows* indicate the months characterized by lowest and highest temperatures correlated to the lighter and heavier isotopes composition, respectively

The elevation effect is also clearly observed. The $\delta^{18}O$ and δD values become lighter with increasing elevation, whereas lower level sites such as rain gauge A (320 m a.s.l.), located at the bottom of the volcanic aquifer (with a mean yearly $\delta^{18}O$ value of –6.9‰ and a mean yearly δD values of –42.1‰) and rain gauge B (520 m a.s.l.; $\delta^{18}O$=–7.5‰, δD=–46.4‰) showed more positive values (Fig. 8). Paternoster et al. (2008) observed a good correlation between the isotopic composition of rainfall and the sample's elevation, defining a gradient of 0.17‰ $\delta^{18}O$/100 m, and 0.84‰ δD/100.

Groundwater isotopic composition: spatial distribution

According to previous studies in many temperate regions, as well as in this study, recharge rates appear to be the highest during winter and early spring when the soils are saturated, and vegetation is dormant (Wenner et al. 1991; Clark and Fritz 1997; Dennis et al. 1997; Winograd et al. 1998; Paternoster et al. 2008). In the Vulture area, recharge is minimal during summer when most of the short-duration and high-intensity rainfall is lost through direct surface runoff and/or is returned to the atmosphere due to the medium-high temperatures and high evapotranspiration rates (Spilotro et al. 2005). This confirms that the main recharge occurs during the winter and spring months.

The average values of the isotopic content in groundwater during the present study ranged from –8 to –10.2‰ for $\delta^{18}O$ and from –53 to –65‰ for δD. The large numbers of stable isotope analyses performed for this study have been reported in Table 3. The observed variations in the measured isotopic values are often within the analytical error ranges ($\delta^{18}O$ and δD are better than 0.8 and 0.10‰, respectively). These isotopic compositions are similar to mean isotopic values detected by Paternoster et al. (2008).

No significant seasonal variation in the isotopic ratios is observed. However, values for a few water points (8, 13, 47 and 48) located in the W–NW sector fall slightly outside of the acceptable analytical error (Fig. 9). These springs show a high degassing rate (bubbling gases by Paternoster 2005) which could results in a shift of the $\delta^{18}O$ isotopic composition towards negative values in the liquid phase. These slightly seasonal fluctuations in the $\delta^{18}O$ and δD values are probably due also to the shorter groundwater flow pathway of the W–NW sector confirming the hydrogeological setting of the considered areas. Under these conditions, it is possible to assume that the hydrological features of the aquifer make the water bodies relatively homogeneous, which, as a consequence, are not influenced by the seasonal variation of the meteoric recharge.

By plotting the mean isotopic composition on a δD vs. $\delta^{18}O$ scattergram, it can be seen (in Fig. 10) that all the samples fall between the Eastern Mediterranean meteoric water line (EMMWL) and the global meteoric water line (GMWL). It is observed that most of the groundwater samples follow the LMWL, in particular fitting the WLMWL (Paternoster et al. 2008) which defines more precisely the meteoric end-member in the local hydrological cycle, providing that the investigated groundwaters are meteoric in origin. However, one sample (sample No. 1, Table 3) is located to the left of the EMMWL, clearly suggesting a depletion in ^{18}O and D (mean values of –10.4 and –59‰, respectively) with respect to the other groundwater samples of the area, and also falling outside of the range defined by the LMWL (Paternoster et al. 2008). The values obtained for this sample would indicate a higher recharge elevation compared with the mean recharge elevations of the other groundwater samples. This difference in $\delta^{18}O$ and δD composition highlights the fact that the hydrological and structural setting probably involves the coexistence of different groundwater flowpaths influencing isotopic groundwater features. The water circulation is probably conditioned by a tectonic structure responsible for the ascent of deeper fluids. As suggested by Paternoster et al. (2008), it is likely that groundwater associated with sample No.1 (see Fig. 10) was recharged under different (e.g. colder) climatic conditions with respect to the present day, justifying the different isotopic values. Secondary processes that occur after the falling of rain such as evaporation and evapotranspiration, do not appear to change the isotope values of groundwater significantly, so that isotope ratios can be used as tracers.

 DOI 10.1007/s10040-010-0619-8

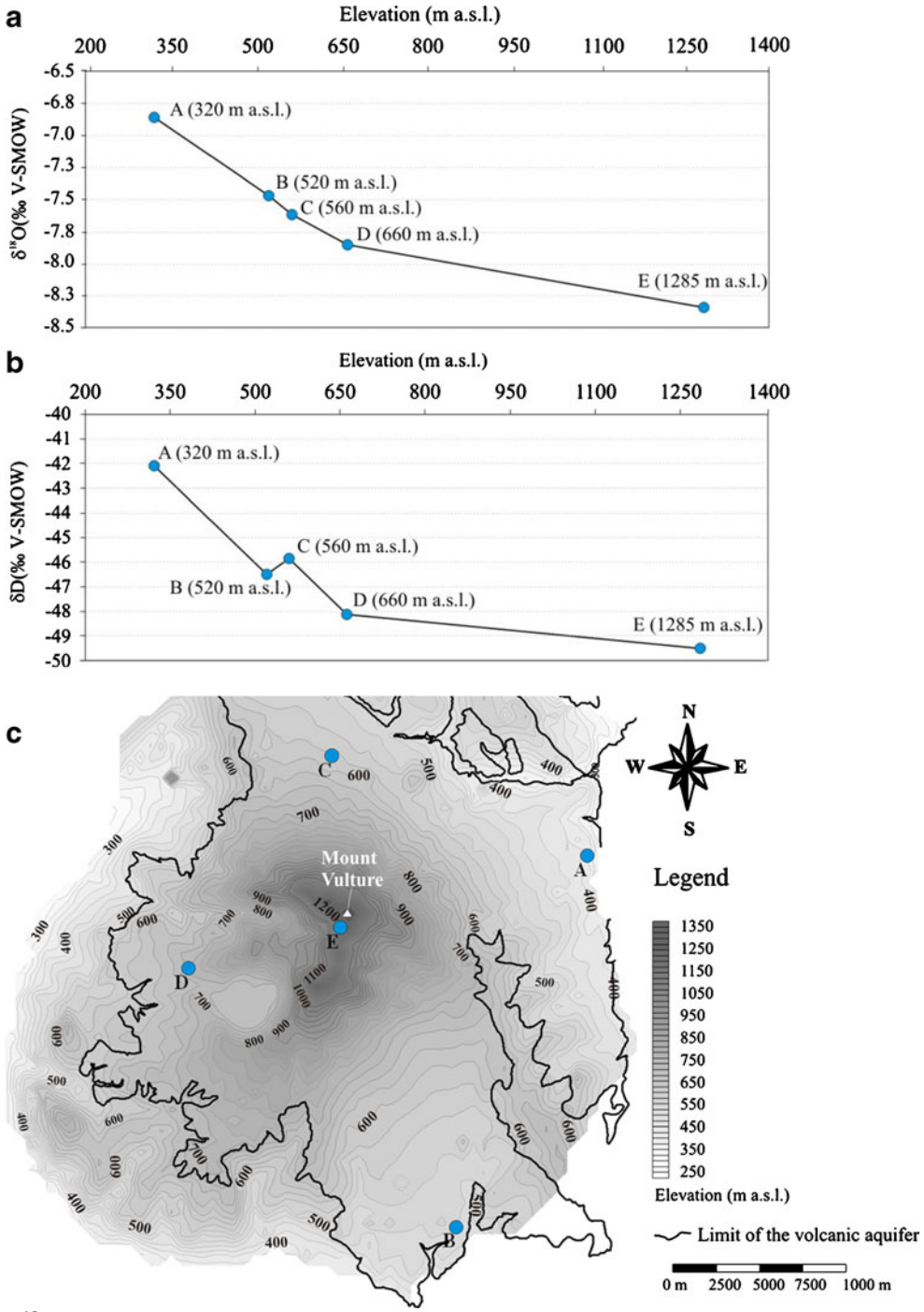

Fig. 8 **a** Plot of $\delta^{18}O$ in rain vs. elevation (m a.s.l.) of the five rain gauge stations (monthly rain samples collected during 2002 by Paternoster et al. 2008); **b** plot of δD in rain vs. elevation (m a.s.l.) of the five rain gauge stations (monthly rain samples collected during 2002 by Paternoster et al. 2008); **c** map showing the location of the rain gauge stations

Figure 11 compares the piezometric map (shown previously in Fig. 4) with the spatial distribution of $\delta^{18}O$ and δD in groundwater, countered using SURFER. As it is possible to note, in some sectors (such as the W–NW and central areas) the shape of the piezometric contours with constant head (Fig. 11a) fits the isotopic contours. This probably indicates that the groundwater flowing in the west-central sector is characterized by shorter flowpaths directly recharged from the rainfall. In the N–NE and S–SE sectors, the shape of the piezometric contours does not show a good fit with the isotopic contours, suggesting a more complex hydrogeological context where the flow-paths are probably longer and deeper than in the W–NW and central areas. The initial isotopic features are slightly modified, probably due to the highest groundwater residence times within the aquifer host rocks.

 DOI 10.1007/s10040-010-0619-8

Table 3 Isotopic composition of each groundwater samplings. The minimum, maximum, and mean values of the three samplings are reported. *NA* not available, wells out of order. The external errors of long-term standard measurements for hydrogen and oxygen are better than 0.8 and 0.10‰, respectively

No.	Sector	Station name	Type	June 2007		February 2008		June 2008		Minimum		Maximum		Mean	
				$\delta^{18}O$ ‰	δD ‰	$\delta^{18}O$ ‰	δD ‰	$\delta^{18}O$ ‰	δD ‰	$\delta^{18}O$ ‰	δD ‰	$\delta^{18}O$ ‰	δD ‰	$\delta^{18}O$ ‰	δD ‰
1	S–SE	Atella F1	Spring	–10.3	–58	–10.8	–60	–10.4	–59	–10.8	–60	–10.3	–58	–10.5	–59
2	S–SE	Atella F3	Spring	–9.0	–57	–9.0	–58	–9.1	–58	–9.1	–58	–9.0	–57	–9.0	–58
3	N–NE	Rapolla 2	Spring	–9.0	–55	–9.2	–54	–9.2	–54	–9.2	–55	–9.0	–54	–9.1	–54
4	N–NE	Rapolla 1	Spring	–8.9	–54	–8.9	–55	–9.0	–55	–9.0	–55	–8.9	–54	–8.9	–55
5	N–NE	Acetosella	Spring	–9.0	–54	–9.0	–55	–8.9	–54	–9.0	–55	–8.9	–54	–9.0	–54
6	W–NW	Pozzo 22 V	Vertical well	–9.3	–57	–9.2	–59	–9.2	–58	–9.3	–59	–9.2	–57	–9.2	–58
7	W–NW	S.Maria de Luco 2	Spring	–8.7	–53	–8.6	–54	–8.6	–54	–8.7	–54	–8.6	–53	–8.6	–54
8	W–NW	Eudria 5	Spring	–9.1	–56	–9.1	–57	–8.5	–57	–9.1	–57	–8.5	–56	–8.9	–57
9	W–NW	Sorgente 34 bis	Horizontal well	–9.1	–54	–9.1	–55	–9.0	–54	–9.1	–55	–9.0	–54	–9.1	–54
10	W–NW	Gaudio 11 V	Vertical well	–9.1	–54	–8.9	–56	–9.1	–54	–9.1	–56	–8.9	–54	–9.0	–55
11	W–NW	Eudria 2	Vertical well	–9.3	–57	–9.3	–57	–9.3	–57	–9.3	–57	–9.3	–57	–9.3	–57
12	W–NW	Pozzo 20 V	Vertical well	–9.3	–56	–9.3	–57	–9.3	–57	–9.3	–57	–9.3	–56	–9.3	–57
13	W–NW	Crocco	Spring	–8.8	–53	–9.1	–54	–8.8	–54	–9.1	–54	–8.8	–53	–8.9	–54
14	W–NW	Sorgente 35	Horizontal well	–9.1	–56	–9.1	–58	–9.1	–56	–9.1	–58	–9.1	–56	–9.1	–57
15	W–NW	S.Maria de Luco 1	Spring	–8.6	–52	–8.7	–53	–8.6	–51	–8.7	–53	–8.6	–51	–8.6	–52
16	S–SE	Nettuno	Horizontal well	–9.1	–57	–9.0	–58	–9.1	–59	–9.1	–59	–9.0	–57	–9.1	–58
17	W–NW	Eudria 3	Spring	–8.6	–53	–8.6	–54	–8.6	–53	–8.6	–54	–8.6	–53	–8.6	–53
18	W–NW	Eudria 4	Spring	–9.0	–53	–9.0	–53	–8.9	–52	–9.0	–53	–8.9	–52	–9.0	–53
19	W–NW	Sorgente 36	Horizontal well	–9.4	–56	–9.3	–57	–9.3	–56	–9.4	–57	–9.3	–56	–9.3	–56
20	W–NW	Pozzo 23 V	Vertical well	–9.0	–59	–9.1	–60	–9.0	–59	–9.1	–60	–9.0	–59	–9.0	–59
21	W–NW	Eudria 1	Spring	–8.5	–55	–8.4	–57	–8.4	–56	–8.5	–57	–8.4	–55	–8.4	–56
22	S–SE	Atella 2	Spring	–8.3	–53	–8.2	–54	–8.2	–53	–8.3	–54	–8.2	–53	–8.2	–53
23	S–SE	Fonte Itala 1	Vertical well	–9.1	–55	–9.0	–56	–9.0	–55	–9.1	–56	–9.0	–55	–9.0	–55
24	N–NE	Giovanna	Vertical well	–9.1	–58	–9.1	–59	n.a	n.a	–9.1	–59	–9.1	–58	–9.1	–59
25	N–NE	Angelicchio	Vertical well	–9.0	–59	–9.2	–60	–9.0	–59	–9.2	–60	–9.0	–59	–9.1	–59
26	W–NW	Gaudio 21 V	Vertical well	–9.0	–54	–9.1	–56	–9.2	–54	–9.2	–56	–9.0	–54	–9.1	–55
27	S–SE	Fonte Itala 2	Horizontal well	–8.7	–59	–8.7	–59	–8.7	–59	–8.7	–59	–8.7	–59	–8.7	–59
28	W–NW	Pozzo 24 V	Vertical well	–9.0	–57	–9.1	–59	–9.1	–58	–9.1	–59	–9.0	–57	–9.1	–58
29	S–SE	Pozzo 4	Vertical well	–8.5	–55	–8.5	–56	–8.5	–55	–8.5	–56	–8.5	–55	–8.5	–55
30	S–SE	San Marco	Horizontal well	–8.2	–54	–8.3	–56	–8.3	–55	–8.3	–56	–8.2	–54	–8.3	–55
31	W–NW	Pozzo 15 V	Vertical well	–9.4	–55	–9.3	–56	–9.3	–55	–9.4	–56	–9.3	–55	–9.3	–55
32	S–SE	Pozzo 3	Vertical well	–8.5	–53	–8.6	–54	–8.7	–54	–8.7	–54	–8.5	–53	–8.6	–54
33	N–NE	Pozzo D	Vertical well	–8.6	–53	–8.7	–54	–8.8	–53	–8.8	–54	–8.6	–53	–8.7	–53
34	S–SE	Pozzo 5	Vertical well	–8.9	–57	–8.8	–57	–8.8	–57	–8.9	–57	–8.8	–57	–8.8	–57
35	S–SE	Pozzo A	Vertical well	–9.0	–57	–8.9	–59	–9.0	–57	–9.0	–59	–8.9	–57	–9.0	–58
36	S–SE	Pozzo B	Vertical well	–8.8	–55	–8.9	–57	–8.9	–55	–8.9	–57	–8.8	–55	–8.9	–56
37	N–NE	Pozzo 2	Vertical well	–9.1	–54	–9.1	–56	–9.0	–55	–9.1	–56	–9.0	–54	–9.1	–55
38	W–NW	Fontana dei Faggi	Spring	–9.3	–56	–9.4	–57	–9.3	–57	–9.4	–57	–9.3	–56	–9.3	–57
39	W–NW	Piloni	Spring	–9.4	–58	–9.5	–59	–9.5	–59	–9.5	–59	–9.4	–58	–9.5	–59
40	S–SE	Fonte Tripoli	Spring	–8.2	–54	–8.2	–55	–8.2	–54	–8.2	–55	–8.2	–54	–8.2	–54
41	S–SE	Pozzo Dilva	Vertical well	–8.5	–56	–8.5	–56	–8.5	–56	–8.5	–56	–8.5	–56	–8.5	–56
42	S–SE	Sorgente Bosco Bufara	Spring	–8.6	–56	–8.5	–56	–8.5	–56	–8.6	–56	–8.5	–56	–8.5	–56
43	N–NE	Savino	Vertical well	–9.4	–56	–9.6	–56	–9.6	–56	–9.6	–56	–9.4	–56	–9.5	–56
44	S–SE	Sveva 2	Vertical well	–9.2	–52	NA	n.a	–9.4	–51	–9.4	–52	–9.2	–51	–9.3	–52
45	S–SE	Sveva	Vertical well	–8.0	–52	NA	n.a	–8.0	–51	–8.0	–52	–8.0	–51	–8.0	–52
46	S–SE	Lilia 2	Vertical well	–9.2	–54	–9.2	–55	–9.3	–54	–9.3	–55	–9.2	–54	–9.2	–54
47	W–NW	Toka	Vertical well	–8.0	–50	NA	n.a	–8.7	–50	–8.7	–50	–8.0	–50	–8.4	–50
48	W–NW	Solaria	Vertical well	–8.0	–51	–8.6	–53	n.a	n.a	–8.6	–53	–8.0	–51	–8.3	–52

Discussion: recharge and discharge patterns of the Mt. Vulture volcanic aquifer system

The recharge elevation was calculated using the equation relating elevation and isotope ratios of precipitation with isotopic gradients of the Mt. Vulture area (–0.17‰ for $\delta^{18}O$/100 m and –0.84‰ for δD/100 m) reported by Paternoster et al. (2008). Recharge elevations for groundwater at the sampling points were calculated by resolving the Paternoster equation ($\delta^{18}O‰$=–0.0017 H –7.28), with

 DOI 10.1007/s10040-010-0619-8

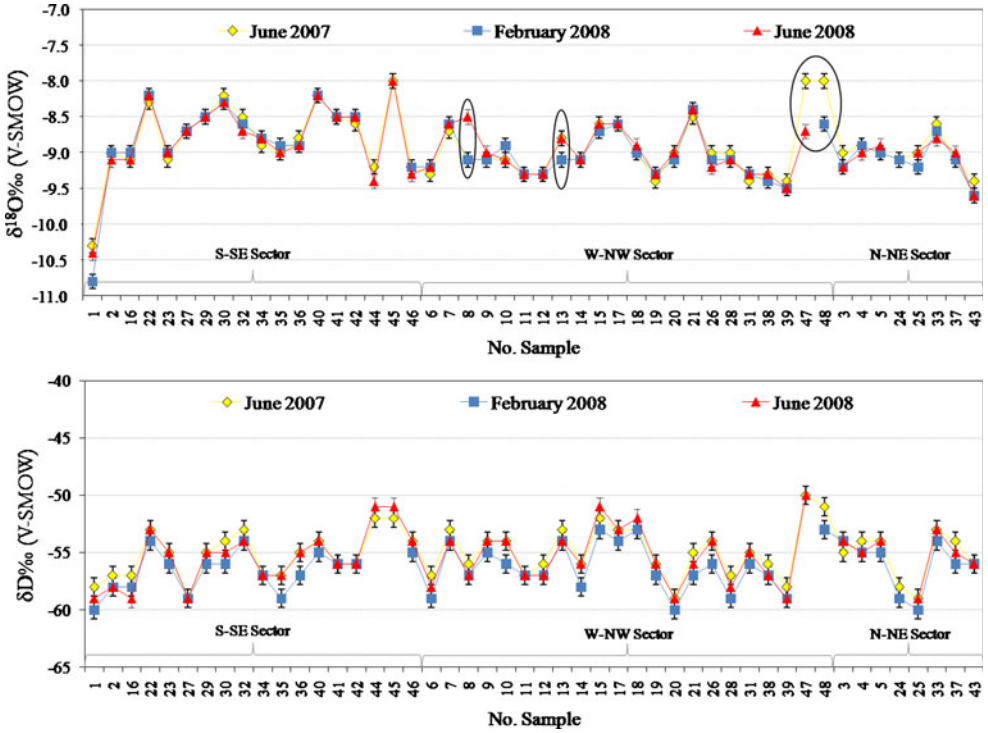

Fig. 9 Seasonal fluctuation of the groundwater isotopic compositions listed in Table 3. *Error bar*s for each sample are ±0.1‰ for $\delta^{18}O$ and ±0.8‰ for δD. Sample numbers (*No. Sample*) are as given in Table 3 but arranged by sector. The *circled values* falling slightly outside of the acceptable analytical error are relative to the springs which show a high degassing rate resulting in a shift of the $\delta^{18}O$ isotopic composition towards negative values in the liquid phase

elevation (*H*) defining the corresponding $\delta^{18}O$ values of the sampling points. The mean inferred recharge elevations are compiled (Table 4) and illustrated in Fig. 12. The measured elevations represent the spring elevations and the water-table elevations (m a.s.l.) of the shallow and deep wells.

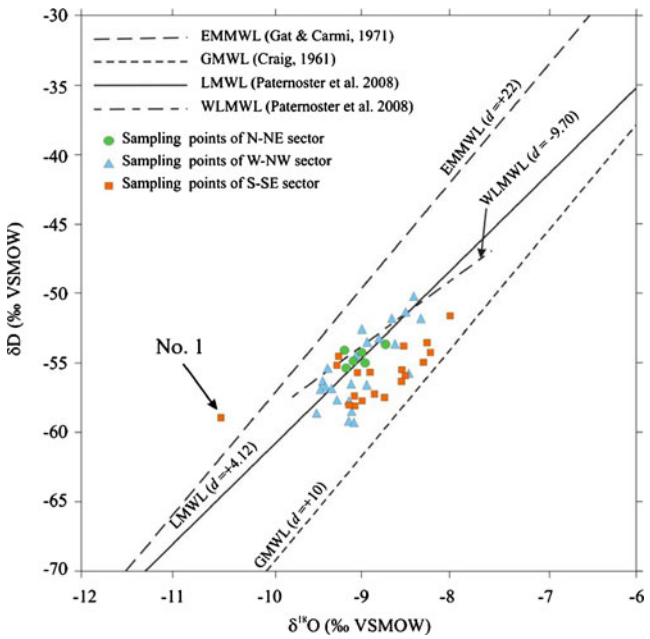

Fig. 10 Isotopic groundwater values of Mt. Vulture area. Global meteoric water line (*GMWL*) from Craig (1961); Eastern Mediterranean meteoric water line (*EMMWL*) from Gat and Carmi (1971); Local meteoric water line (*LMWL*) from Paternoster et al. (2008); Weighted local meteoric water line (*WLMWL*) from Paternoster et al. (2008)

From the computed inferred recharge elevations (Fig. 12), three different sectors were defined to improve the conceptual hydrogeological model of the studied area. The sampling points of the S–SE sector, located at the bottom of the volcanic aquifer at low elevations (between 394 and 450 m a.s.l.), show an inferred mean recharge elevation ranging from 555 to 1,300 m a.s.l., which occur in the high and medium elevations of the area close to Mt. San Michele and Mt. Vulture (Fig. 13). The S–SE sector has an inferred mean recharge elevation that suggests a remote recharge area with relatively long residence times. The inferred recharge elevations of some sampling points (1, 2, 44 and 46; see Fig. 13) do not seem to be compatible with the local radial flow system shown by the water-table map of Fig. 4. In fact, there is a large difference between the water-table elevation and the estimated mean elevation of the recharge area. The water isotopic composition could result from a mixing of shallow and deep waters, probably influenced by tectonic structures, controlling groundwater flowpaths in the discharge area belonging to a deeper aquifer that was recharged under different (e.g. colder) climatic conditions with respect to the present day (Paternoster et al. 2008).

The N–NE sector represents a minor discharge sector where the recharge area of the outflow points show an inferred elevation ranging from 900 to 1,300 m a.s.l., where spring and well water-table elevations range between 300 and 530 m a.s.l. Therefore, the N–NE sector

 DOI 10.1007/s10040-010-0619-8

is characterized by shorter groundwater flowpaths than the S–SE sector. In contrast, the W–NW sector of the Vulture aquifer shows mean inferred recharge elevations, ranging from 700 to 1,300 m a.s.l., compatible with the measured elevations of the springs and well water levels.

Based on this study, the S–SE and N–NE sectors represent the principal out-flowing areas where the deeper groundwater discharge is, respectively, about 7 and 3 km away (Fig. 13). In the W–NW sector, which represents the main recharge area, the groundwater flows are characterized by shorter flowpaths. Some springs discharge locally derived groundwater that circulates at shallow depths in the subsurface.

By using the mean inferred-recharge elevation obtained from the integrated isotopic analysis, it is possible to show graphically the recharge and discharge patterns to give a simplification of the conceptual hydrogeological model of the groundwater flowpaths in the investigated area (Fig. 13). The integration of the isotopic and hydraulic data with hydrogeochemical analysis, permits the hydrogeochemical tracing of the groundwater flows in the Mt. Vulture volcanic aquifer.

Concluding remarks

The integrated study of the rainwater isotopic composition and groundwater hydrogeochemical and isotopic characteristics of the Mt. Vulture area have highlighted the following points:

1. The geochemical characteristics of groundwater found in the investigated aquifer show heterogeneity among different sectors. The two identified hydrogeochemical water types reflect the water–interaction processes taking place within the host aquifer rocks.

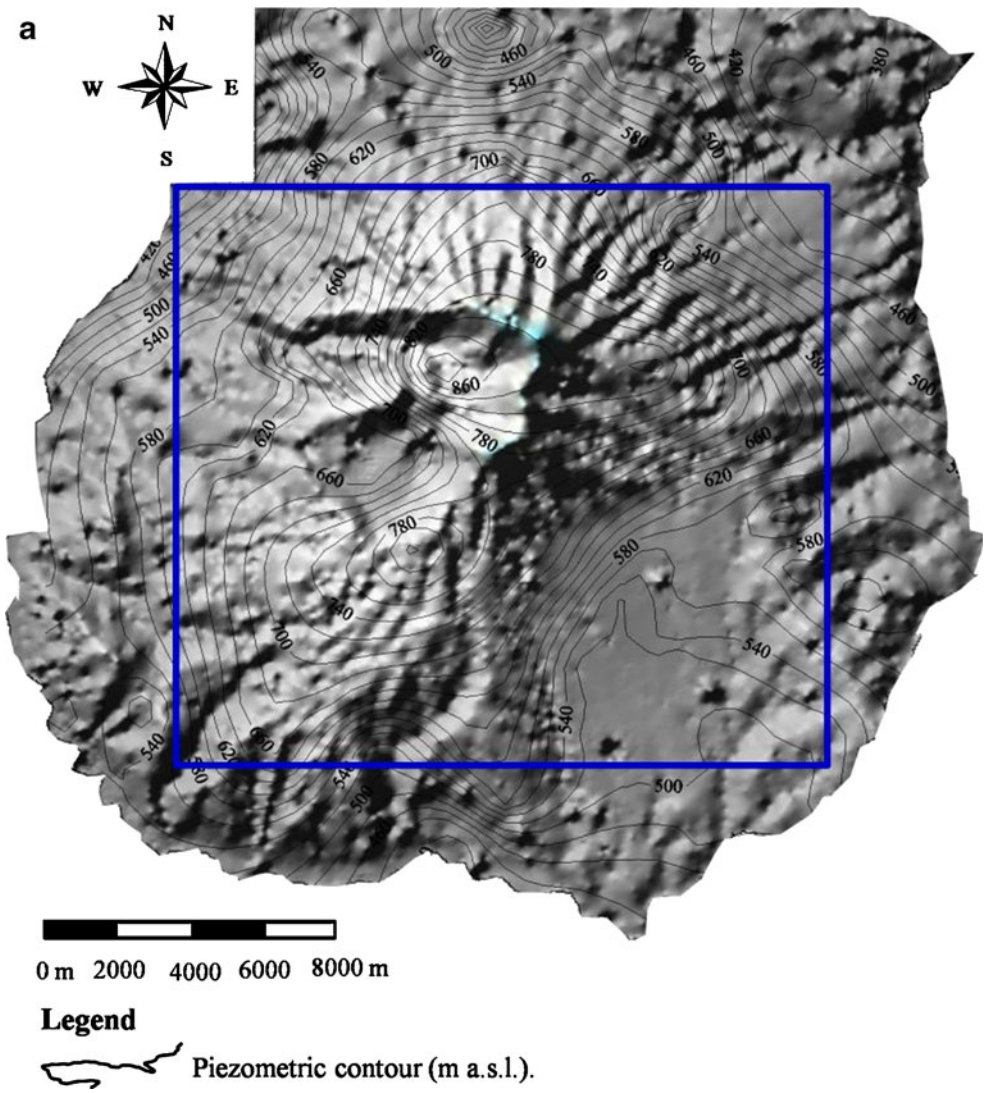

Fig. 11 Isotopic contour maps drawn (using SURFER). **a** shows the piezometric surface contours and the area delineated in (**b**) and (**c**). Contour maps for **b** $\delta^{18}O$ and **c** δD in groundwater samples; *blue circles* indicate the sampling points; *blue lines* indicate the volcanic aquifer limit. The map and the location data are provided in UTM Zone 33 coordinates, using the European Datum of 1950

 DOI 10.1007/s10040-010-0619-8

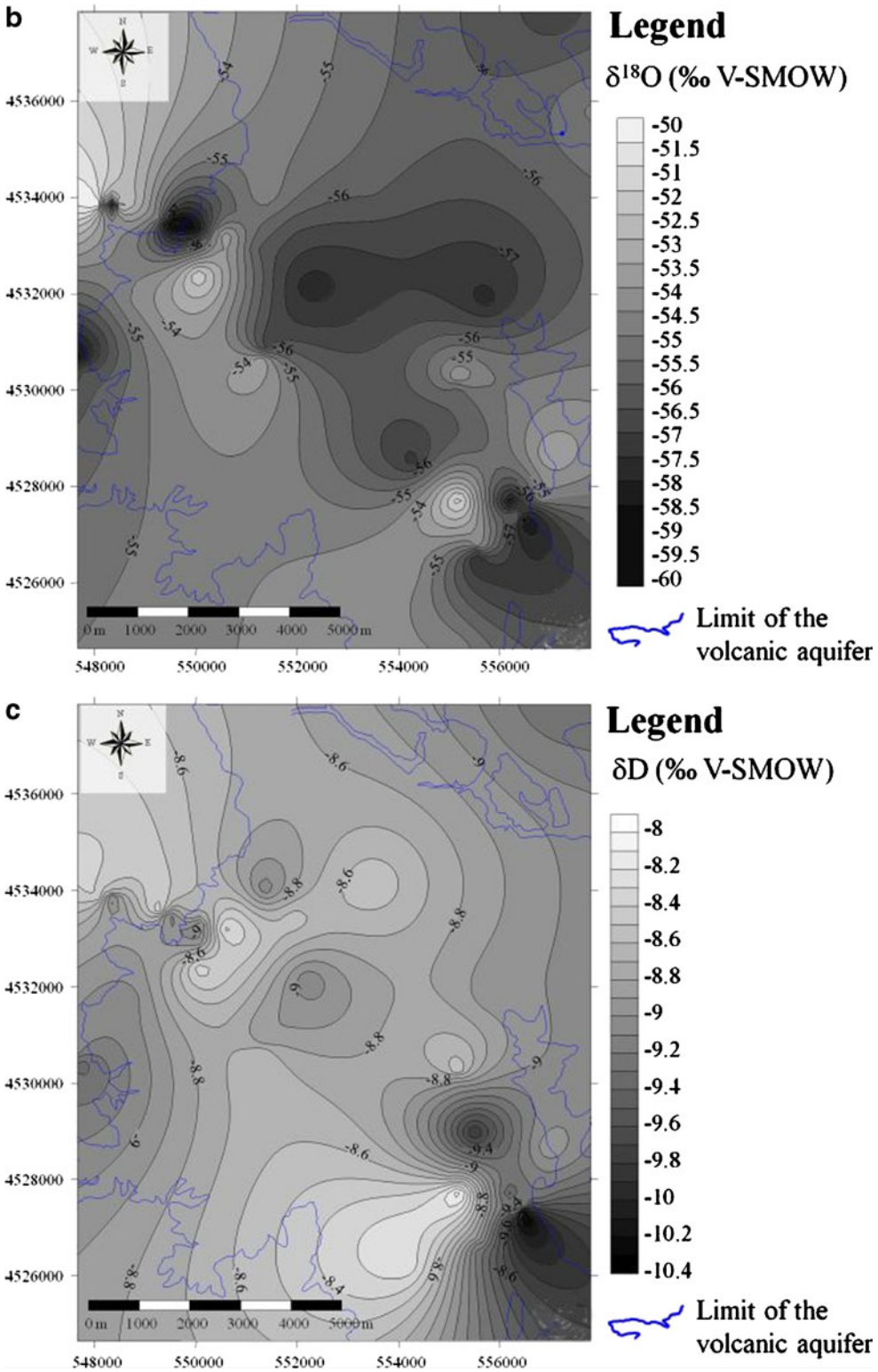

Fig. 11 (continued)

2. The original composition of the recharge rainwater is modified by low–temperature leaching of the host volcanic rocks. The chemical results show the occurrence of two distinct groundwater types. The first water type displays a bicarbonate alkaline–earth composition. The second water type, flowing in the N–NE and principally in the S–SE sectors, displays a sulphate-bicarbonate composition with the highest Na and SO_4 contents, possibly related to their circulation in fluvio-lacustrine deposits, with intercalations of feldspathoid-

 DOI 10.1007/s10040-010-0619-8

Table 4 Inferred recharge elevation computed using the equation relating elevations and isotope ratios of precipitation with isotopic gradients of Mt. Vulture area (–0.17 and –0.84‰ for $\delta^{18}O$/100 and δD/100 m, respectively) reported by Paternoster et al. (2008). For explanation see reported text. The table contains measured spring and well water-level elevations

No.	Station name	$\delta^{18}O$‰	Measured spring elevation (m a.s.l.)	Measured well water-level elevation (m a.s.l.)	Inferred recharge elevation (m a.s.l.)
S–SE SECTOR					
1	Atella F1	–10.5	461	-	1,345
2	Atella F3	–9.0	394	-	1,020
16	Nettuno	–9.1	-	487	1,050
22	Atella 2	–8.2	474	-	570
23	Fonte Itala 1	–9.0	-	490	1,010
27	Fonte Itala 2	–8.7	-	490	825
29	Pozzo 4	–8.5	-	545	725
30	San Marco	–8.3	-	490	585
32	Pozzo 3	–8.6	-	541	740
34	Pozzo 5	–8.8	-	544	910
35	Pozzo A	–9.0	-	600	990
36	Pozzo B	–8.9	-	626	940
40	Fonte Tripoli	–8.2	488	-	555
41	Pozzo Dilva	–8.5	-	493	720
42	Bosco Bufara	–8.5	449	-	725
44	Sveva 2	–9.3	-	554	1,280
45	Sveva	–8.0	-	527	615
46	Lilia 2	–9.2	-	552	1,130
W–NW SECTOR					
6	Pozzo 22 V	–9.2	-	690	1,140
7	S.Maria de Luco 2	–8.6	519	-	780
8	Eudria 5	–8.9	551	-	960
9	Sorgente 34 bis	–9.1	-	657	1,050
10	Gaudio 11 V	–9.0	-	644	1,025
11	Eudria 2	–9.3	547	-	1,180
12	Pozzo 20 V	–9.3	-	650	1,195
13	Crocco	–8.9	575	-	960
14	Sorgente 35	–9.1	-	566	1,060
15	S.Maria de Luco 1	–8.6	515	-	800
17	Eudria 3	–8.6	558	-	740
18	Eudria 4	–9.0	554	-	985
19	Sorgente 36	–9.3	-	565	1,215
20	Pozzo 23 V	–9.0	-	682	1,045
21	Eudria 1	–8.4	547	-	700
24	Giovanna	–9.1	-	813	1,060
25	Angelicchio	–9.1	-	820	1,060
26	Gaudio 21 V	–9.1	-	735	1,060
28	Pozzo 24 V	–9.1	-	780	1,065
31	Pozzo 15 V	–9.3	-	555	1,210
38	Fontana dei Faggi	–9.3	885	-	1,210
39	Piloni	–9.5	960	-	1,290
47	Toka	–8.4	-	396	660
48	Solaria	–8.3	-	643	680
N–NE SECTOR					
3	Rapolla 2	–9.1	360	-	975
4	Rapolla 1	–8.9	352	-	915
5	Acetosella	–9.0	365	-	1,240
33	Pozzo D	–8.7	352	-	900
37	Pozzo 2	–9.1	-	686	1,000
43	Savino	–9.5	-	535	1,300

rich pyroclastic layers. This different composition is due to the complex geological and hydrogeological contexts of the aquifer.

3. Using the isotopic gradient (0.17‰ for $^{\delta 18}O$/100 m), three main sectors within the Mt. Vulture hydrogeological system can be distinguished:

   – The W–NW sector, which constitutes the main recharge area of the studied aquifer, showing an isotopic signature similar to rainwater. The slightly seasonal fluctuations of a few water points, characterized by the occurrence of a high degassing rate (bubbling gases), could results in a shift of the $\delta^{18}O$ isotopic composition towards negative values in the liquid phase. These slightly seasonal fluctuations in the $\delta^{18}O$ values are probably also due to the shorter groundwater flowpath of the W–NW sector, confirming the hydrogeological setting of the considered areas. The recharge contributing to groundwater appears to be derived from a mean

 DOI 10.1007/s10040-010-0619-8

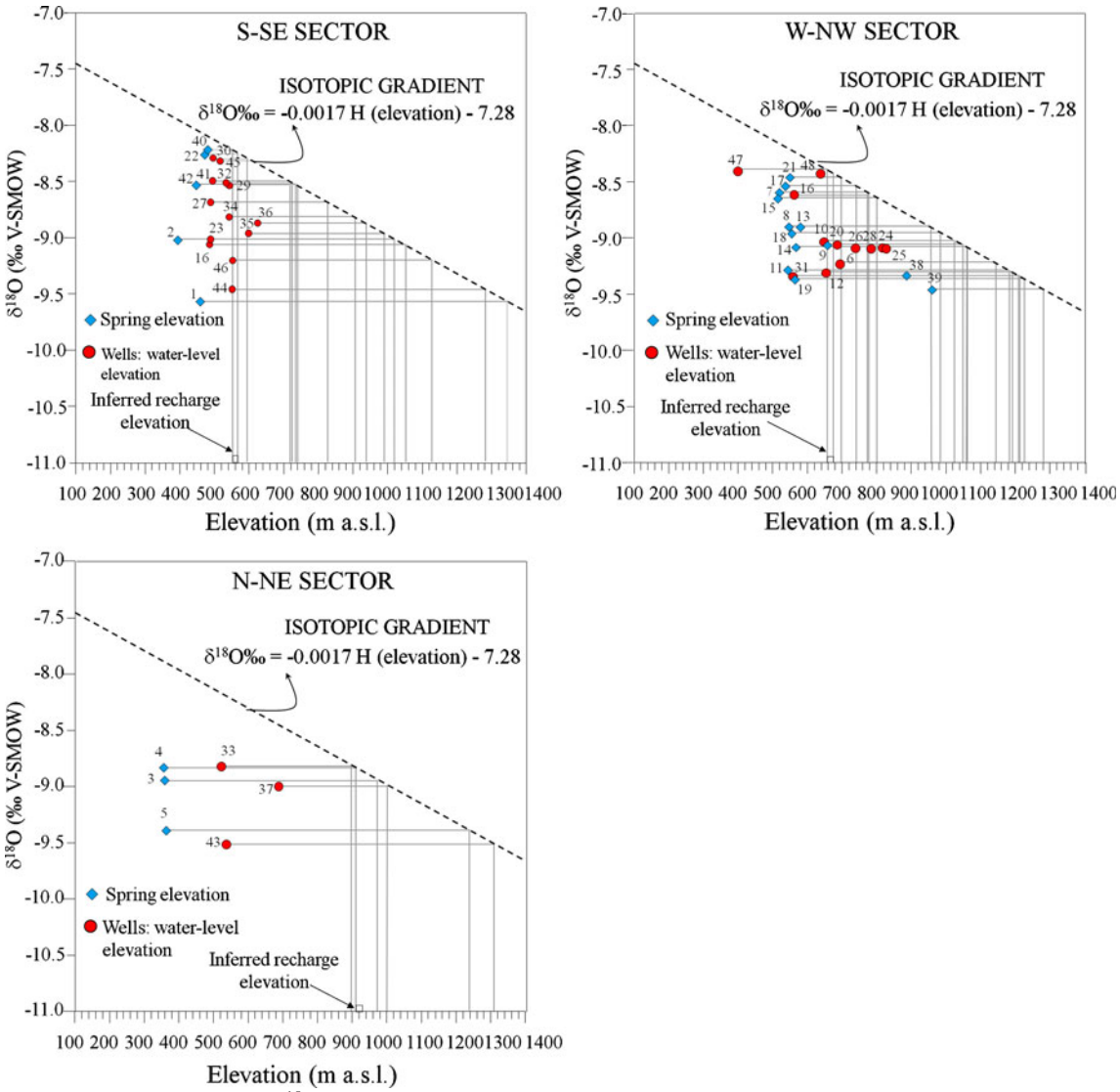

Fig. 12 Inferred recharge elevations. $\delta^{18}O$ values of springs and groundwater vs. elevation. The *dotted line* and the equation represent the regression line of δ^{x}, where x = O measurements in precipitation at different elevations from Paternoster et al. (2008)

elevation ranging from 700 to 1,100 m a.s.l., close to the measured elevation of the springs and well water levels.

– The second and third sectors represent the main discharge areas toward the S–SE and N–NE areas respectively. No evidence for seasonal variation of the groundwater isotopic composition was observed. The mean elevation of the recharge area of the deeper groundwater is about 1,100 m a.s.l. which is a hydrologically reasonable value for the Mt. Vulture area. This implies that the deeper waters that are recharged at higher elevations have longer flowpaths. This confirms that most flow in the Mt. Vulture region conforms to the radial pattern, but from the highest to the lowest elevations there are some irregularities in the flow. Based on this study, the S–SE and S–SE sectors represent the principal out-flowing areas where the deeper groundwater discharge is derived from about 5 km away.

4. This investigation improved the previous conceptual hydrogeological model proposed by Spilotro et al. (2005, 2006), which, at large scale, defined the radial streamlines of the groundwater flowpath. The present hydrogeochemical, hydraulic and integrated isotopic study allowed better definition of the recharge and discharge patterns of the Mt. Vulture volcanic aquifer system. By means of this study, the W–NW area, at the highest elevations, was found to be the main recharge

 DOI 10.1007/s10040-010-0619-8

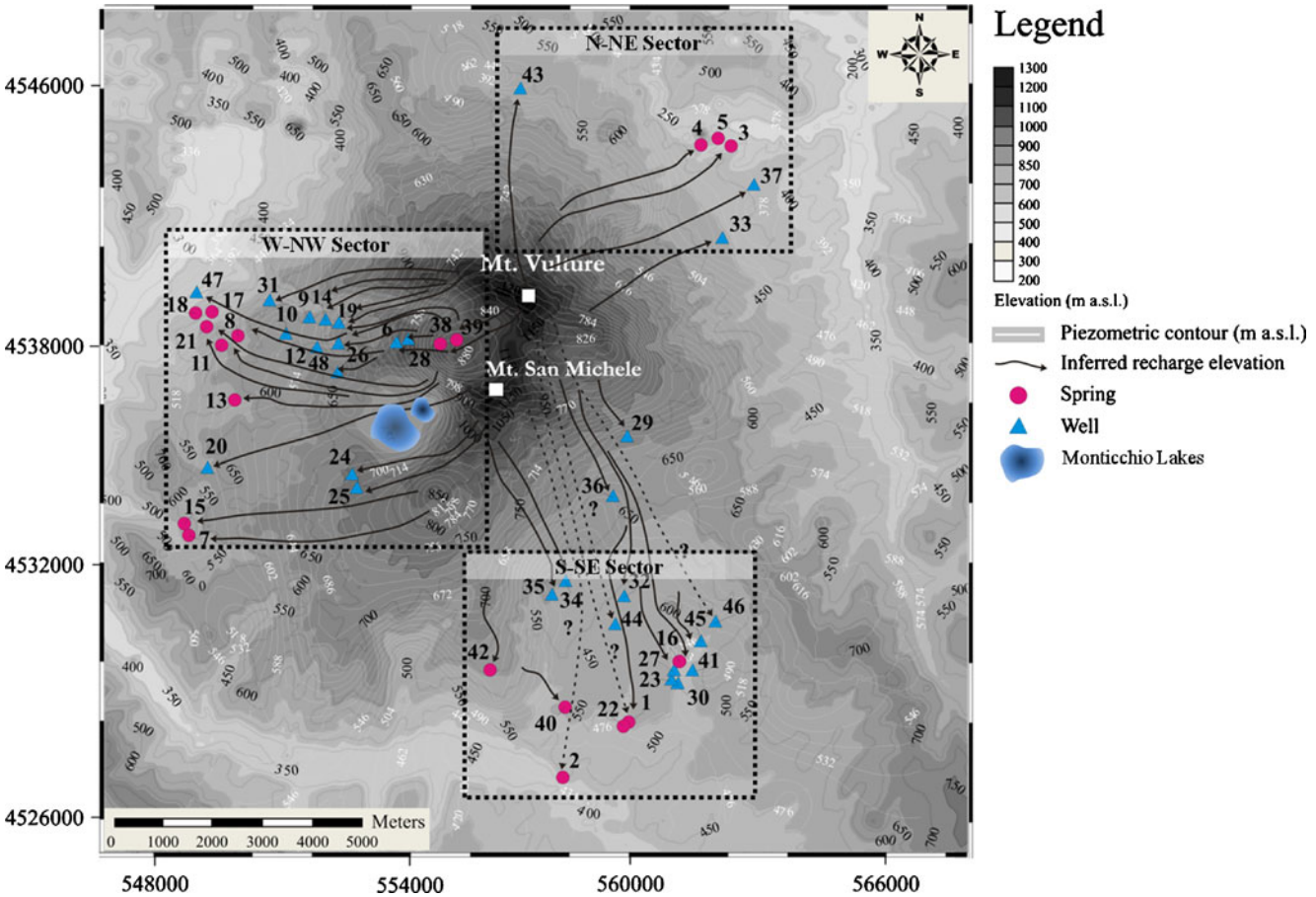

Fig. 13 Recharge and discharge patterns of the Mt. Vulture volcanic aquifer system. The map and the location data are provided in UTM Zone 33 coordinates, using the European Datum of 1950. *Rectangles with dashed black line* show the three main sectors within the Mt. Vulture hydrogeological system. The S–SE and N–NE sectors are discharge areas; the W–NW sector is a recharge area. *Question mark* on the *dashed flow lines* shows that recharge elevations are uncertain. Mt. Vulture and Mt. San Michele are the main places of the investigated area

area close to the drainage axis (Grigi Valley-Fosso del Corbo fault), widely affecting the preferential groundwater flow, where several operating wells of companies and private owners are located. The flowing groundwater moves along radial flowpaths toward the lowest elevations in the S–SE and S–SE sectors but with differences in length and depth. This fact is supported also by the groundwater hydrogeochemical differences from the highest to the lowest elevations of the volcanic aquifer.

As mentioned previously, several hydrogeochemical and stable isotope studies have been performed to characterize recharge and discharge processes in quite simple hydrogeological environments. The studies in volcanic aquifers were found to be more complex. The complex hydrogeochemical characteristics of groundwater at a volcanic site have resulted in the development of stable-isotope and chemical-tracer tools for investigating recharge processes and groundwater flow pathways of these hydrogeological systems. Given the importance of the studied area, the present investigation can be useful to the studies of volcanic aquifers comparable to the Mt. Vulture system.

The presented work can contribute to policies of conservation and management, also with time-based criteria, in sensitive recharge areas which should be protected for drinking-water supply and other uses. Therefore, this study may be used as an aid in regional planning to establish groundwater management rules.

Acknowledgements This report was, in reference to the PhD Thesis by S. Parisi, supported in part by the Department of Hydrogeology of Freie Universität, Berlin, Germany. We wish to thank the Alfred Wegner Institute of Potsdam, Germany, for their scientific and technical support during the development of this work. The authors gratefully acknowledge comments on a draft manuscript by Editor Philippe Renard and Associate Editor Sam Earman. We also appreciate review comments by Manuel Nathenson and an anonymous reviewer, all of which led to significant improvements in the manuscript.

References

Annunziatellis A, Beaubien SE, Bigi S, Ciotoli G, Coltella M, Lombardi S (2008) Gas migration along fault systems and through the vadose zone in the Latera caldera (central Italy): implications for CO_2 geological storage. Int J Greenhouse Gas Control 2:353–372

Barbieri M, Boschetti T, Pettita M, Tallini M (2005) Stable isotope (^{2}H, ^{18}O and $^{87}Sr/^{86}Sr$) and hydrochemistry monitoring for groundwater hydrodynamics analysis in a karst aquifer (Gran Sasso, central Italy). Appl Geochem 20:2063–2081

Beneduce P, Giano SI (1996) Osservazioni preliminari sull'assetto morfostrutturale dell'edificio vulcanico del M. Vulture (Basilicata) [Preliminary observations on the morpho-structural features of the M. Vulture volcanic edifice (Basilicata)]. Quat Ital J Quat Sci 9(1):325–330

Boenzi F, La Volpe L, Rapisardi L (1987) Evoluzione geomorfologica del complesso vulcanico del M. Vulture (Basilicata) [Geomorphological evolution of the Mt. Vulture volcanic complex (Basilicata)]. Boll Soc Geol Ital 106:673–682

Bonardi G, Ciarcia S, Di Nocera S, Matano F, Sgrosso I, Torre M (2009) Carta delle principali unità cinematiche dell'Appennino meridionale: nota illustrativa [Map of the principal kinematic units of the southern Apennines: explanatory notes]. Boll Soc Geol Ital 128(1):47–60

Brocchini D, La Volpe L, Laurenzi MA, Principe C (1994) Storia evolutiva del M. Vulture [Evolutionary history of Mt. Vulture]. Plinius 12:22–25

Buettner A, Principe C, Villa IM, Brocchini D (2006) Geocronologia ^{39}Ar-^{40}Ar del Monte Vulture [Geochronology ^{39}Ar-^{40}Ar of the Monte Vulture]. In: C. Principe (a cura di) La Geologia del Monte Vulture. Regione Basilicata. Dipartimento Ambiente, Territorio e Politiche della Sostenibilità. Grafiche Finiguerra, Lavello, Italy, pp 73–86

Caracausi A, Favara R, Nicolosi M, Nuccio PM, Paternoster M (2009) Gas hazard assessment at the Monticchio crater lakes of Mt. Vulture, a volcano in southern Italy. Terra Nova. doi:10.1111/j.1365-3121.2008.00858.x

Celico P, Summa G (2004) Idrogeologia dell'area del Vulture (Basilicata) [Hydrogeology of the Vulture area (Basilicata)]. Boll Soc Geol Ital 123:343–356

Ciccacci S, Del Gaudio V, La Volpe L, Sansò P (1999) Geomorphological features of Monte Vulture Pleistocene Volcano (Basilicata, southern Italy). Zeitschrift Geomorphol N.F. (Suppl. Bd.) 114:29–48

Clark I, Fritz P (1997) Environmental isotopes in hydrogeology. Lewis, Boca Raton, FL

Cook PG, Herczeg AL (2000) Environmental tracers in subsurface hydrology. Kluwer, Boston, MA

Craig H (1961) Isotopic variation in meteoric waters. Science 133:1702–1203

D'Alessandro W, Federico C, Longo M, Parello F (2004) Oxygen isotope composition of natural waters in the Mt. Etna area. J Hydrol 296(1–4):282–299

Dansgaard W (1964) Stable isotopes in precipitation. Tellus 16:436–467

Dennis F, Andrews JN, Parker A, Poole J (1997) Isotopic and noble gas study of Chalk groundwater in the London Basin, England. Appl Geochem 12:763–773

Gat JR, Carmi H (1971) Evolution of the isotopic composition of atmospheric waters in the Mediterranean Sea area. J Geophys Res 75:3039–3040

Giannandrea P, La Volpe L, Principe C, Schiattarella M (2004) Carta geologica del Monte Vulture alla scala 1:25.000 [Geological map of Monte Vulture, scale 1:25.000]. Litografia Artistica Cartografica, Florence, Italy

Giannandrea P, La Volpe L, Principe C, Schiattarella M (2006) Unità stratigrafiche a limiti inconformi e storia evolutiva del vulcano medio-pleistocenico di Monte Vulture (Appennino meridionale, Italia) [Unconformity-bounded stratigraphic units and the evolutionary history of the middle Pleistocene Monte Vulture volcano (southern Apennine, Italy)]. Boll Soc Geol Ital 125:67–92

Jones IC, Banner JL (2003) Estimating recharge thresholds in tropical karst island aquifers: Barbados, Puerto Rico and Guam. J Hydrol 278:131–143

La Volpe L, Patella D, Rapisardi L, Tramacere A (1984) The evolution of the Monte Vulture volcano (southern Italy): inferences from volcanological, geological and deep dipole electrical soundings data. J Volcanol Geotherm Res 22:147–162

Lee KS, Wenner DB, Lee IS (1999) Using H-and O-isotopic data for estimating the relative contributions of rainy and dry season precipitation to groundwater: example from Cheju Island, Korea. J Hydrol 222:65–74

Liotta M, Brusca L, Grassa F, Inguaggiato S, Longo M, Madonia P (2006) Geochemistry of rainfall at Stromboli volcano (Aeolian Islands): isotopic composition and plume–rain interaction. Geochem Geophys Geosyst 7:Q07006. doi:10.1029/2006GC001288,Issn:1525-2027

Marfia AM, Krishnamurthy RV, Atekwana EA, Panton WF (2003) Isotopic and geochemical evolution of ground and surface waters in a karst dominated geological setting: a case study from Belize, Central America. Appl Geochem 19:937–946

Marini L, Paiotti A, Principe C, Ferrara G, Cioni F (1994) Isotopic ratio and concentration of sulfur in the undersaturated alkaline magmas of Vulture Volcano (Italy). Bull Volcanol 56:487–492

Meyer H, Schönicke L, Hubberten WH, Fridrichsen H (2000) Isotope studies of hydrogen and oxygen in ground ice? Experiences with the equilibration technique. Isot Environ Health Stud 36:133–149

Nathenson M, Thompson JM, Withe LD (2003) Slightly thermal springs and non-thermal springs at Mount Shasta, California: chemistry and recharge elevations. J Volcanol Geoth Res 121:137–153

Paternoster M (2005) Mt. Vulture volcano (Italy): a geochemical contribution to the origin of fluids and to a better definition of its geodynamic setting. PhD Thesis, University of Palermo, Italy, pp 1–92

Paternoster M, Liotta M, Favara R (2008) Stable isotope ratios in meteoric recharge and groundwater at Mt. Vulture volcano, southern Italy. J Hydrol 348:87–97

Paternoster M, Parisi S, Caracausi A, Favara R, Mongelli G (2009) Groundwaters of Mt. Vulture volcano, southern Italy: chemistry and sulfur isotope composition of dissolved sulfate. Geochem J 43(2):125–135

Principe C, Giannandrea P (2002) Stratigrafia ed evoluzione geologica del vulcano Vulture (Basilicata, Italia). (Rapporti fra vulcanismo ed ambienti sedimentari) [Stratigraphy and geological evolution of the Vulture volcano (Basilicata, Italy): relationship between volcanic event and sedimentary environments]. In: Cinematiche collisionali: tra esumazione e sedimentazione. 81° riunione estiva della Società Geologica Italiana, Torino, 10–12 September 2002, abstract volume, pp 280–281

Reed MJ (1983) Introduction. In: Reed MJ (ed) Assessment of low-temperature geothermal resources of the United States-1982. US Geol Surv Circ 892, pp 1–8

Regione Basilicata (1987) Allegato 5.1. Catasto dei corpi idrici. Ai sensi della legge n. 319/1976 e successivi aggiornamenti. Schede delle sorgenti (1° e 2°) 1° fase [Attachment 5.1. Land register of the hydrological bodies. Regional law No. 319/1976. Springs Database]. Landsystem S.p.A., Rome

Regione Basilicata (1989) Progetto di piano di risanamento delle acque. Volume IV. Censimento dei corpi idrici. Schede dei Corpi Idrici: Laghi, Bacini e Serbatoi, Corsi d'Acqua, Acque Costiere, Acque di Transizione, Pozzi [Recovery plan for the groundwater, vol IV: census of the hydrological bodies. Database of the hydrological bodies: lakes, basins and groundwater reservoirs, coastal groundwater, transitional groundwater, Wells]. Landsystem S.p.A., Rome

Schiattarella M, Beneduce P, Giano SI, Giannandrea P, Principe C (2005) Assetto strutturale ed evoluzione morfotettonica quaternaria del vulcano del Monte Vulture (Appennino Lucano) [Structural setting and Quaternary morpho-tectonic evolution

of the Monte Vulture volcano (Lucan Apennine)]. Boll Soc Geol Ital 124:543–562

Scholl MA, Gingerich SB, Tribble GW (2002) The influence of microclimates and fog on stable isotope signatures used in interpretation of regional hydrology: East Maui, Hawaii. J Hydrol 264:170–184

Serri G, Innocenti F, Manetti P (2001) Magmatism from Mesozoic to Present: petrogenesis, time-space distribution and geodynamic implications In: Vai GB, Martini IP (eds) Anatomy of an orogen: the apennines and adjacent Mediterranean basins. Kluwer, Dordrecht, The Netherlands, pp 77–104

Spilotro G, Canora F, Caporale F, Caputo R (2000) Piano di Tutela e Sviluppo del Bacino Idrominerario del Monte Vulture [Safeguard and development plan of the Mount Vulture hydromineral basin]. Regione Basilicata report, Regione Basilicata, Potenza, Italy

Spilotro G, Canora F, Caporale F, Caputo R, Fidelibus MD, Leandro G (2005) Idrogeologia del M. Vulture (Basilicata, Italia) [Hydrogeology of M. Vulture (Basilicata, Italy)]. Paper presented at: Aquifer Vulnerability and Risk, 2nd International Workshop, 4th Congress on the Protection and Management of Groundwater, Colorno, Italy, September 2005

Spilotro G, Canora F, Caporale F, Caputo R, Fidelibus MD, Leandro G (2006) Idrogeologia del Monte Vulture [Hydrogeology of M. Vulture]. In: Principe C (ed) La geologia del Monte Vulture [The geology of the Mount Vulture]. Regione Basilicata, Potenza, Italy, pp 123–132

Stumm W, Morgan JJ (1996) Aquatic chemistry, 3rd edn. Wiley, New York

UNESCO/FAO (1963) Carte bioclimatique de la Zone Méditerrané [Bioclimatic map of the Mediterranean zone]. UNESCO, New York, FAO, Rome

Wenner DB, Ketcham PD, Dowd JF (1991) Stable isotopic composition of waters in a small Piedmont watershed. In: Taylor HP Jr, O'Neil JR, Kaplan IR (eds) Stable isotope geochemistry: a tribute to Samuel Epstein. The Geochemical Society, St. Louis, MO, Spec. Publ. No. 3, pp 195–203

Winograd IJ, Riggs AC, Coplen TB (1998) The relative contributions of summer and cool-season precipitation to groundwater recharge, Spring Mountains, NV, USA. Hydrogeol J 6:77–93

 DOI 10.1007/s10040-010-0619-8